
Theses and Dissertations

Fall 2010

Method for determination of octane rating by flame quenching experiments

Ankush Bhasin
University of Iowa

Copyright 2010 Ankush Bhasin

This thesis is available at Iowa Research Online: <http://ir.uiowa.edu/etd/782>

Recommended Citation

Bhasin, Ankush. "Method for determination of octane rating by flame quenching experiments." MS (Master of Science) thesis, University of Iowa, 2010.
<http://ir.uiowa.edu/etd/782>.

Follow this and additional works at: <http://ir.uiowa.edu/etd>



Part of the [Mechanical Engineering Commons](#)

METHOD FOR DETERMINATION OF OCTANE RATING BY FLAME
QUENCHING EXPERIMENTS

by
Ankush Bhasin

A thesis submitted in partial fulfillment
of the requirements for the Master of
Science degree in Mechanical Engineering
in the Graduate College of
The University of Iowa

December 2010

Thesis Supervisor: Professor Emeritus Lea-Der Chen

Graduate College
The University of Iowa
Iowa City, Iowa

CERTIFICATE OF APPROVAL

MASTER'S THESIS

This is to certify that the Master's thesis of

Ankush Bhasin

has been approved by the Examining Committee
for the thesis requirement for the Master of Science
degree in Mechanical Engineering at the December 2010 graduation.

Thesis Committee: _____
Lea-Der Chen, Thesis Supervisor

Albert Ratner

Ching-Long Lin

ACKNOWLEDGEMENTS

I would like to thank the Graduate College, University of Iowa, for giving me the opportunity to pursue a Master's degree at this university.

I would like to extend my sincere gratitude to my advisor Dr. Lea-Der Chen for his patience, wise advices, brilliant ideas and suggestions and for his strong insistence and high pressure to achieve better work. It was for his wholehearted co-operation, unfailing inspiration and support that I got valuable guidance for carrying out this project successfully.

I would also like to acknowledge ConocoPhillips, partial sponsor of this project. Special thanks to Dr. Garry Gunter and Dr. Sergei Filatyev at ConocoPhillips Technical Center, Bartlesville, OK, for the insightful discussions and support throughout the project.

Special thanks are due to my lab mates - Scott Ruebush and Chris Wong for their assistance and friendship. I wish them best in their lives ahead.

Finally, I am deeply thankful to my family for their patience, endless support and encouragement despite being continents apart.

TABLE OF CONTENTS

LIST OF TABLES	iv
LIST OF FIGURES	v
CHAPTERS	
1. INTRODUCTION AND BACKGROUND	1
1.1 Motivation.....	1
1.2 Objective.....	2
1.3 Background Theory	2
1.3.1 Octane Rating	2
1.3.2 Laminar Premixed Flames	6
1.3.3 Quenching.....	9
2. LITERATURE REVIEW	11
2.1 Flat Flame Research	11
2.2 Octane Number Research	14
2.3 Quenching Research	17
3. EXPERIMENTAL MODEL AND PROCEDURE.....	20
3.1 Experimental Configuration	20
3.2 Methodology.....	26
3.2.1 Safety Procedure.....	28
3.2.2 Experimental Procedure.....	30
3.3 Assitive Computational Study	31
3.3.1 FLUENT	31
3.3.2 CHEMKIN.....	34
4. EXPERIMENTAL RESULTS AND DISCUSSION	43
4.1 Flame Visualization.....	43
4.2 Flame Liftoff.....	50
4.3 Spectrometer	55
4.4 Octane Rating vs. Quenching	63
5. CONCLUSIONS	76
REFERENCES	79

LIST OF TABLES

Table

1.1	Properties of Iso-octane	4
1.2	Properties of N-heptane	5
3.1	Test equipment list with description	23
3.2	Input calculations for iso-octane	26
3.3	Input parameters for PREMIX Flame model	40
4.1	PRF 0 Input conditions for flame visualization	44
4.2	PRF 100 Input conditions for flame visualization	46
4.3	Data for lift-off with PRF 0 and PRF 100 with N ₂ co-flow	64
4.4	Data for lift-off with PRF 65 and PRF 85 with N ₂ co-flow	66
4.5	Data for lift-off with PRF 0 and PRF 100 with He co-flow	68
4.6	Data for lift-off with Gasoline 87 and 91 with N ₂	74

LIST OF FIGURES

Figure	
1.1	Molecular structure of iso-octane3
1.2	Molecular structure of n-heptane4
2.1	Edge-on photograph ($f=3.4$, $1/60$ s) of flat-flame burner fueled by DME: top (ER= 0.67); bottom (ER=1.49). Diameter of flame disk = 6.0 cm.12
2.2	Temperature profiles of the fuel-lean (ER=0.67) and fuel rich (ER=1.49) (left) and fuel lean (ER=0.74) and fuel rich (ER=1.47) (right) atmospheric-pressure DME-air flames plotted as a function of position relative to the burner surface.13
2.3	Computational and experimental results of Kaiser et al. (a) Species mole fractions for the fuel-lean (ER=0.74) methane-air flame plotted as a function of sample probe position (b) Symbols for the experimental data and computed peak concentrations for intermediate species CH_2O (530 ppm); O, C_2H_6 (550 ppm); C_2H_4 (430 ppm); C_2H_2 (30 ppm).....13
2.4	Position of temperature max along reactor length L as a function of ON 1) model mixture; 2) model mixture, differential thermocouple; 3) straight-run naphtha; 4) naphtha frp15
2.5	Unburnt-to-unburnt opposed flow, premixed flame configuration18
3.1	McKenna Flat flame burner22
3.2	Dimensions of McKenna Flat flame burner23
3.3	Experimental test arrangement24
3.4	3D mesh of burner model31
3.5	Temperature contours projected on plane perpendicular to burner base32
3.6	Velocity vectors of flame, nitrogen and surrounding air33
3.7	Particle traces colored by x-component velocity (m/s)33
3.8	Temperature profiles as a function of distance above burner for PRF 0, 50 and 100 at ER =1.0 with 122 grid point solution36
3.9	OH mole concentrations as a function of distance above burner for PRF 0 and 100 at ER = 1.0 with 122 grid point solution37
3.10	Laminar burning velocities (left) and adiabatic flame temperatures (right) versus ER for syngas compositions: 1) 5% H_2 , 95% CO 2) 50% H_2 , 50% CO 3) 95% H_2 , 5% CO.....40

3.11	Laminar burning velocities (left) and adiabatic flame temperatures (right) versus ER for landfill gas compositions: 1) 100% CH ₄ , 0% CO ₂ 2) 90% CH ₄ , 10% CO ₂ 3) 55% CH ₄ , 45% CO ₂	41
3.12	Laminar burning velocities (left) and adiabatic flame temperatures (right) versus ER for gasification gas compositions: 1) 24% CO, 21% H ₂ , 55% N ₂	42
4.1	Flame images for premixed n-heptane fuel at the given equivalence ratios.....	44
4.2	Flame images for premixed iso-octane fuel at the given equivalence ratios	47
4.3	Flame image for premixed PRF 80 at the ER =1.51.....	48
4.4	Flame images for premixed toluene fuel at the given equivalence ratios.....	49
4.5	Flame lift off images for PRF 0 with nitrogen co-flow	52
4.6	Flame lift off images for PRF 100 with nitrogen co-flow	54
4.7	Flame images from spectrometer for n-heptane with no nitrogen co-flow	55
4.8	Flame images from spectrometer for iso-octane with no nitrogen co-flow.....	57
4.9	Flame images from spectrometer for n-heptane with nitrogen co-flow	58
4.10	Flame images from spectrometer for iso-octane with nitrogen co-flow.....	59
4.11	Flame images from spectrometer for PRF 0 and PRF 100 at ER = 1.51 showing difference in lift of at wavelengths of 475 nm and 550 nm	60
4.12	Flame images from spectrometer for PRF 0 and PRF 100 at ER = 2.01 at wavelength of 425 nm.....	61
4.13	Flame images from spectrometer for toluene with nitrogen co-flow	62
4.14	Lift-off with nitrogen vs. equivalence ratio for PRF 0, 100	65
4.15	Lift-off with nitrogen vs. equivalence ratio for PRF 0, 65, 85 and 100	67
4.16	Lift-off with helium vs. equivalence ratio for PRF 0, 100	70
4.17	Difference in lift-off with N ₂ and He as secondary gas velocity for PRF 0 and 100	72
4.18	Lift-off with N ₂ as shield gas velocity for Gasoline 87 and 91, PRF 0 and 100	73
4.19	Lift-off with N ₂ as shield gas velocity for Gasoline 87 and 91, PRF 0 and 100 with lines along with symbols	75

CHAPTER 1: INTRODUCTION AND BACKGROUND

1.1 Motivation

Since the development of internal combustion engines, inventions have been made to improve their efficiency. One of the primary aspects of which is to develop the understanding of the relationship between the engine and fuel that burns within it. In particular, the fuel's propensity to auto-ignite is an important characteristic which can dictate the ability of an engine to work to its full thermodynamic potential. Fuel is desired to ignite rapidly after injection into the combustion chamber when working with the compression-ignition engine (CI). However, in a spark-ignition (SI) engine, a high resistance to auto-ignition is favored mainly to prevent knocking. Knocking is an unwanted ringing sound caused by auto-ignition of the fuel/air mixture ahead of the turbulent flame front. Effects of engine knocking range from inconsequential to completely destructive and acts as the main limiting factor of thermodynamic efficiency. The methods employed by the industries today in determining the octane rating of gasoline fuels is by taking a composition of iso-octane and n-heptane which would have the same knocking behavior and compare it to the fuel which is run through a test engine with controlled conditions. The purpose of this investigation was to develop a correlation between octane number and optically measurable characteristics of a premixed flame using thermal quenching process.

There are numerous numerical and experimental studies to find correlations of octane rating with fuel properties. This thesis was based on the hypothesis that quenching characteristics at ignition locations impact the flame development. Conversely, determination of quenching characteristics might serve as an effective measure to determine the fuel mixture octane number. This hypothesis was tested with premixed

flame experiments using primary reference fuels (iso-octane and n-heptane) and commercial grade gasoline.

1.2 Objective

The main purpose of this research was to determine whether or not quenching experiments can be used to determine octane numbers of fuel-air mixtures. Premixed flame experiments were conducted on a flat flame burner. Primary reference fuels of different ratios were taken and correlated to their respective thermal quenching condition by introducing co-flowing inert gasses at room temperature with fuel-air mixture. The inert gasses that were used in the experiment are nitrogen and helium and the results are analyzed using a camera and an imaging spectrometer. The key objective was to find the distinction in lift off or quenching of flames when higher octane number fuels were used compared to when lower octane number fuels were employed.

1.3 Background Theory

1.3.1: Octane Rating

In 1927 the knock rating was introduced by Graham Edgar as a measure for the knock resistance of a fuel. He suggested using the ratio of two hydrocarbons that could be produced in sufficient purity and quantity for reference purposes. He also defined the knock ratings of these two standard substances: 0 for the unbranched (n-heptane) and 100 for the branched-chain hydrocarbon (2, 2, 4-trimethyl pentane, iso-octane). By this method the knock proneness of gasolines with different compositions became measurable by their comparison to corresponding standard mixtures with the same knock resistance. Simultaneously a quantitative result of the measurement was produced in form of the 'octane number' (ON). The octane rating is a measure of the resistance of fuels to auto

ignition. It was developed by chemist Russell Marker at the Ethyl Corporation in 1926. The mixture of iso-octane and n-heptane gives an octane number to a fuel. It is defined by the percentage volume of iso-octane present in the mixture. For example, a mixture with 80% iso-octane and 20% n-heptane would have an octane number of 80. This mixture is called the primary reference fuel and it is considered to have the same anti-knocking capacity of the fuel such as petrol under test. This does not mean that the petrol contains just iso-octane and heptane in these proportions, but that it has the same detonation resistance properties. There are some fuels which have higher knock-resistant properties than iso-octane, hence the definition is extended to allow for octane numbers higher than 100. In other words, it is a measure of the fuel's tendency to burn in a controlled manner, rather than exploding in an uncontrolled manner.

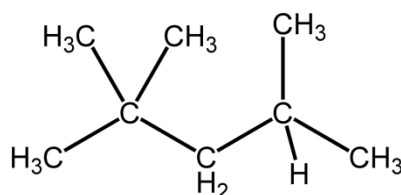


Figure 1.1: Molecular structure of iso-octane

Iso-octane (2, 2, 4-trimethylpentane) is an octane isomer which defines the 100 point on the octane rating scale. It is produced on a massive scale in the petroleum industry, usually as a mixture with related hydrocarbons. Table 1.1 shows some basic properties of iso-octane relative to this study.

Table 1.1: Properties of Iso-octane

Molecular formula	C ₈ H ₁₈
Molar mass	114.2 g/mol ⁻¹
Appearance	Colorless liquid
Density	688.0 kg/m ³ , liquid
Melting point	-107.4 C, 166.0 K, -161.0 F
Boiling point	99.3 C, 372.0 K, 211.0 F

N-heptane is the straight-chain alkane with the chemical formula H₃C(CH₂)₅CH₃ or C₇H₁₆. When used as a test fuel component in anti-knock test engines, a 100% heptane fuel is the zero point of the octane rating scale. It is undesirable in petrol, because it burns explosively, causing engine knocking, as opposed to branched-chain octane isomers, which burn more slowly and give better performance. It was chosen as the zero point of the scale because of the availability of very high purity n-heptane, unmixed with other isomers of heptane or other alkanes, distilled from the resin of Jeffery Pine and from the fruit of *Pittosporum resiniferum*. Following is the structure and basic properties of n-heptane.

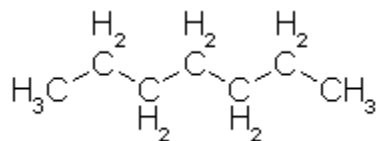


Figure 1.2: Molecular structure of n-heptane

Table 1.2: Properties of N-heptane

Molecular formula	C_7H_{16}
Molar mass	100.2 g/mol^{-1}
Appearance	Colorless liquid
Density	0.684 g/ml , liquid
Melting point	-90.6 C , 182.5 K
Boiling point	98.4 C , 371.6 K

The two methods that are employed for octane number testing are called the Research Octane number (RON) and Motor Octane Number (MON). These are measured under two differing engine conditions in a standard “Cooperative Fuels Research” (CFR) engine which has a variable compression ratio, a fuel metering system which easily adjusts the fuel–air ratio and a “knock meter” which gives a value of the “knocking intensity” based on the pressure rise rate in arbitrary units between 0 and 100. Test conditions for RON test involves an engine speed of 600 rpm, intake temperature of 52 C and spark timing of 13. MON is considered as the better measure of how the fuel behaves when under load as it is done at a higher engine speed of 900 rpm. MON testing uses a similar test engine to that used in RON testing, but with a preheated fuel mixture at about 149 C, a higher engine speed, and variable ignition timing (21-14) to further stress the fuel's knock resistance. Depending on the composition of the fuel, the MON of a modern gasoline will be about 8 to 10 points lower than the RON. In many countries, including United States, average of RON and MON is taken that is called the Anti-Knock Index (AKI), and often written on pumps as $(R+M)/2$). It may also sometimes be called the Road Octane Number (RdON), Pump Octane Number (PON), or $(R+M)/2$.

It is advised that fuels with higher octane ratings should be used in more powerful engines, since such fuels ignite less easily, which seems unusual as higher octane ratings correlate to higher activation energies. Activation energy is the amount of energy necessary to start a chemical reaction. Since higher octane fuels have higher activation

energies, it is less likely that a given compression will cause auto-ignition. Therefore, the reason higher octane rating fuels are advised for powerful engines as an uncontrolled ignition is not desired in a spark ignition engine.

1.3.2: Laminar Premixed Flames

A flame is a self-sustaining propagation of a localized combustion zone at subsonic velocities. There are several key terms in this definition. For flame to be localized, it means that the flame occupies only a small portion of the combustible mixture at any one time. Second, a discrete combustion wave that travels subsonically is termed as deflagration. Combustion waves also propagate at supersonic velocities and such a wave is called detonation. Some of the principal characteristics of laminar premixed flames include adiabatic flame temperature, flame speed and flame thickness. The flame speed is the measured rate of expansion of the flame front in a combustion reaction. In other words, it is the speed at which a laminar flame propagates through a pre-mixture of fuel and air. In an internal combustion engine, the flame speed of a fuel is a property which determines its ability to undergo controlled combustion without detonation. Flame speed is used along with adiabatic flame temperature to help determine the engine's efficiency.

Theories of laminar flames have occupied many researchers for many decades. Simplified and detailed analysis of the flame has been laid out coupling principles of heat transfer, mass transfer, chemical kinetics and thermodynamics to understanding the factors governing flame speed and thickness. Numerical simulations have also been performed on laminar premixed flames that employ both detailed chemical kinetics and mixture transport properties. Apart from the steady propagation of premixed laminar flames, the essential transient processes involve concepts of flame quenching and ignition. Although the processes are transient, this study will bind to examining limit

behavior. i.e., conditions under which a flame will either extinguish or not, and ignore the time-dependent details of the extinction and ignition processes.

Flame stabilization is an essential term in premixed laminar flames and involves some key concepts. Important design criteria for gas burners are the avoidance of flashback and lift-off. If the flame propagates back towards upstream of the burner, the phenomenon is called flashback. Flashback will happen if the reactant flow rate sustaining a laminar premixed flame is significantly reduced or shut-off and the passageways upstream of the flame are larger than the quenching distances. Lift-off is the condition where flame is not attached to the burner tube or port but, rather, is stabilized at some distance from the port. The phenomena of flashback and lift-off are both related to matching the local laminar burning velocity to the local flow velocity. Flashback is generally a transient event, occurring as the fuel flow is decreased or turned off. When the local flame speed exceeds the local flow velocity, the flame propagates upstream through the tube or port. When the fuel is stopped, flames will flashback through any tubes or ports that are larger than the quenching distance. Therefore, we expect the controlling parameters for flashback to be the same as those affecting quenching, e.g., fuel type, equivalence ratio, flow velocity, and burner geometry. Flame lifting depends on a local flame and flow properties near the edges of the burner port. On a circular tube at low flow velocities the edge of the flame lies quite close to the burner lip and is said to be attached. When the velocity is increased, the cone angle of the flame decreases in accordance with the condition given in equation below and the edge of the flame is displaced a small distance downstream. With further increases in the flow velocity, a critical velocity is reached where the flame edge jumps to this position, it is said to be lifted. Increasing the velocity beyond the lift-off value results in increasing the lift-off distance until the flame abruptly blows off the tube altogether.

$$\alpha = \sin^{-1} S_L / v_u$$

where, α is the angle of the flame with the burner surface, S_L is the laminar burning velocity and v_u is the velocity of the unburnt mixture.

In this study, flame is quenched by employing a certain method to create a liftoff. This is presented in more detail in the following chapters. Lift-off and blowoff can be explained by the countervailing effects of decreased heat and radical loss to the burner tube and increased dilution with ambient fluid, which occur as the flow velocity is increased. Considering a flame that is stabilized quite close to the burner rim, the local flow velocity at the stabilization location is small as a result of the boundary layer that develops in the tube. The velocity at the wall inside the tube is zero. Both heat and reactive species diffuse to the wall because of the close proximity of the flame to the cold wall, causing the local laminar burning velocity at the stabilization point also to be small. With the flame speed and flow velocities equal and of relatively small magnitude, the flame edge lies close to the burner tube. When the flow velocity is increased, the flame anchor point moves downstream; however the flame burning velocity increases since the heat/radical losses are less because the flame is now not as close to the cold wall. This increase in the burning velocity results in only a small downstream adjustment, and hence the flame remains attached. With further increases in the flow velocity, another effect becomes important that is the dilution of the mixture with ambient fluid as a result of diffusion. Since dilution tends to offset the effects of less heat loss, the flame lifts. With further increases in flow velocity, a point is reached at which there is no location across the flow at which the local flame speed matches the flow velocity and the flame blows off the tube.

1.3.3: Quenching

Quenching in terms of combustion refers to extinguishing a flame. There are many ways in which a flame can be extinguished. A flame can be extinguished by thermal effects (heat loss), chemical suppression and aerodynamic effects. One of the main researched areas is quenching by a cold wall. Premixed flames get extinguished upon entering sufficiently small passageways. This involves the critical diameter of a tube or critical distance between two flat plates through which a flame will not propagate and is called the quenching distance. Radical termination is another way by which a flame could be quenched. The new chemical is added to the fuel line which contains scavengers of certain species present in the flame. These are called flame inhibitors. They inhibit the flame by reducing the burning velocity of premixed flames. The inhibition is characterized by several gas-phase radical recombination cycles that proceed at nearly gas-collisional rates. Hence, burning velocity measurements become an important first step in assessing an inhibitor's effectiveness and testing mechanism performance.

Influence of strain and stretch rate on structures of premixed flames is another form of quenching that is being researched upon. The state of strain of the flow field within a laminar flame, and the magnitude of possible energy exchanges with its surroundings, are both important factors which control properties such as its extinction limits, or the completeness of combustion within the flame. The studies performed by Law et al. (1986) on the influence of strain rate on laminar premixed methane-air flames have shown that, on the whole, the flame speed increases linearly with increasing strain rate. The topic of flame strain has been discussed by many authors, as referenced by Dixon-Lewis (1990). As described by Matalon (1983), normally strain is not uniform over a flame surface, but is defined locally at a point, and instantaneously. Nevertheless, there are three well-known examples where the strain rate is uniform over the whole of any isothermal surface in the flame. Two of these are the spherical and the uniform flow

cylindrical cases mentioned previously. The third is the counter flow or stagnation-point flow configuration. The study on quenching using a counter flow configuration is described in the literature review section that highlights quenching.

Thermal quenching is the process where a flame is quenched because of temperature differences between two mediums. The quenching medium could be a cooler surface or wall as mentioned above or an inert gas at relatively lower temperature than the flame. This is the primary method used in this study to create lift-off of premixed flames. It is done to correlate different fuel mixtures quenching capabilities to their specific octane rating.

CHAPTER 2: LITERATURE REVIEW

2.1 Flat Flame Research

McKenna Flat burners are widely used in the combustion community for producing flat premixed flames. These flames are considered as standards for the development and calibration of optical techniques. Rich premixed flames produced by McKenna burners are frequently investigated both by optical and by sampling techniques. Measurements are normally performed along the axis of the flames, with a uniform distribution of temperature and species concentration assumed in the radial direction. The flame is assumed to be one-dimensional and considered as a standard, at least under lean and close-to stoichiometric conditions. The burner is employed in many laboratories around the world for the development and calibration of optical diagnostic techniques.

Kaiser et al. (2000) made use of the flat flame McKenna burner for measuring chemical species profiles at atmospheric pressure for two dimethyl ether (DME)-air flat flames. This study also focused on the ignition characteristics of the fuel and related those to flame characteristics and properties in the following way. Compression-ignition (diesel) engines require fuels that ignite easily. The ignition efficiency is defined by the cetane number of the fuel, which must be relatively high ($> 40-50$) for a good diesel fuel. The high cetane rating that characterizes DME (>50) is in contrast to the very low cetane rating of branched ethers such as methyl tert-butyl ether (MTBE), which are difficult to ignite by compression and are used as octane enhancers in spark ignition engine fuels. Hence, DME serves as an important alternative diesel fuel because of its dramatic differences in ignition characteristics. This creates the need to study oxidation chemistry of DME. To explore the high temperature oxidation chemistry of DME further, Kaiser et al. measured the chemical species profiles of two DME flames (fuel-rich and fuel-lean) stabilized on a flat-flame burner at atmospheric pressure. In addition, they obtained

chemical species profiles in rich and lean methane-air flames of similar fuel to air ratio for comparison to the DME experiments. These experimental profiles are compared to profiles generated in a computer modeling study using the best available DME-air chemical kinetic mechanism. Apart from using the sampling probe as a measuring device for the thickness of the luminous zone, Kaiser et al. (2000) also used a digital camera with an aperture of $f = 3.4$ and a shutter speed of $1/60$ seconds to verify the probe-based measurement. These photographs were used to estimate the thickness and the brightness of the flames. A typical photograph for a flame is displayed in Figure 2.1. Similar flame images are studied in this research project using a high definition camera. Modeling simulations were carried out using CHEMKIN III with the PREMIX package and with HCT (Hydrodynamics Chemistry and Transport) modeling code which was made compatible to CHEMKIN format. The experimental temperature profiles versus distance above the burner (Figure 2.2) were used as input in the simulation of these flames.

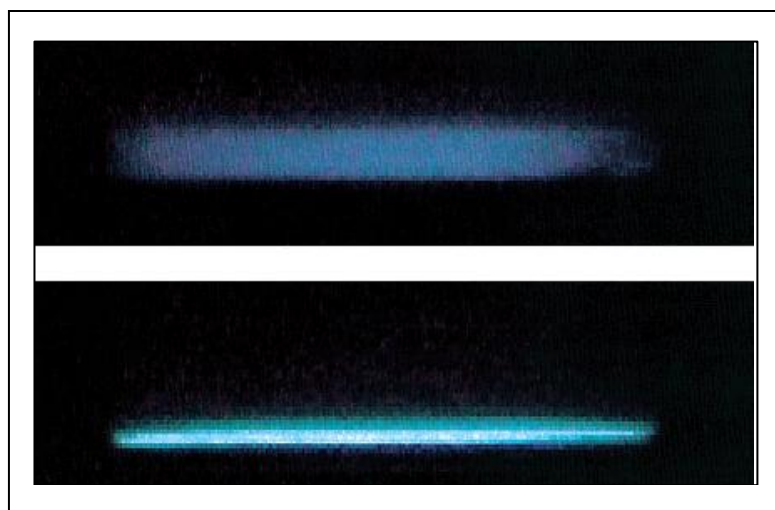


Figure 2.1: Edge-on photograph ($f=3.4$, $1/60$ s) of flat-flame burner fueled by DME: top (ER= 0.67); bottom (ER=1.49). Diameter of flame disk = 6.0 cm.

Source: Kaiser et al. (2000) "Experimental and Modeling Study of Premixed Atmospheric-Pressure Dimethyl Flames", J. Phys. Chem. A 2000, 104, 8194-8206

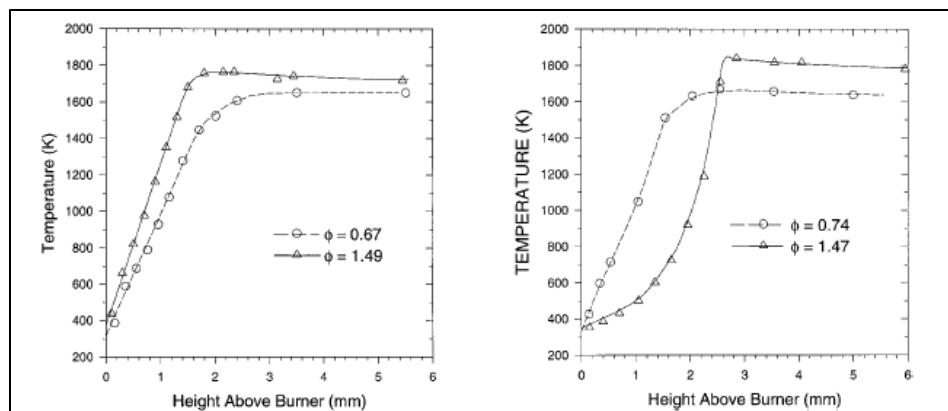


Figure 2.2: Temperature profiles of the fuel-lean (ER=0.67) and fuel rich (ER=1.49) (left) and fuel lean (ER=0.74) and fuel rich (ER=1.47) (right) atmospheric-pressure DME-air flames plotted as a function of position relative to the burner surface

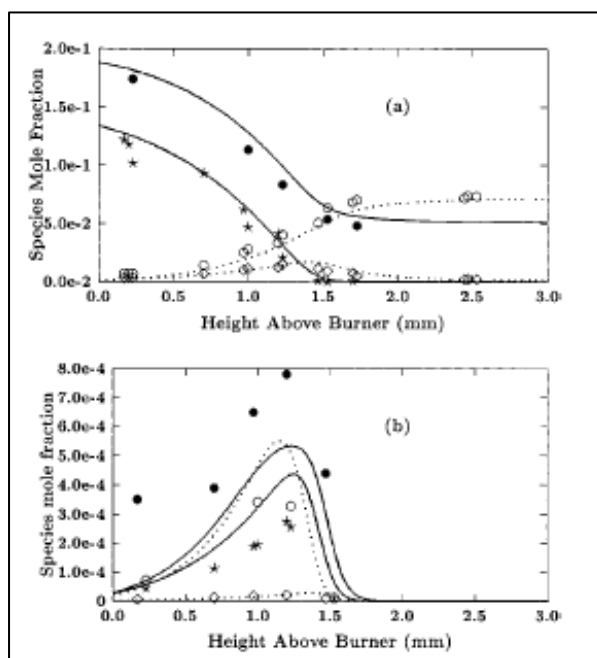


Figure 2.3: Computational and experimental results of Kaiser et al. (a) Species mole fractions for the fuel-lean (ER=0.74) methane-air flame plotted as a function of sample probe position (b) Symbols for the experimental data and computed peak concentrations for intermediate species CH_2O (530 ppm); O , C_2H_6 (550 ppm); C_2H_4 (430 ppm); and C_2H_2 (30 ppm)

Source: Figure 2.2-2.3: Kaiser et al. (2000) "Experimental and Modeling Study of Premixed Atmospheric-Pressure Dimethyl Flames", J. Phys. Chem. A 2000, 104, 8194-8206

Finally, comparisons of the experimentally measured and computationally predicted species profiles versus the distance above burner for the DME flames were made which had a good agreement.

The flat flame burner has also been employed for the calibration of laser thermometry techniques by Hartung et al. (2006). They developed a variety of diagnostic techniques which allow the exploration of a wide range of combustion parameters, e.g. temperature, species concentrations and flow fields. Such techniques are most usefully calibrated in well-characterized laminar flames, where temperature, concentration and flow patterns are stationary and can be predictably controlled. Over the last few decades several burner types have been developed in this context. The commercially available McKenna burner has been the most commonly applied calibration burner for laser diagnostic applications and is characterized by a flat flame. Cheskis et al. (2009) studied the laser spectroscopy diagnostics of low pressure flames using the McKenna burner and produced methods that provide very important information for the creation and validation of chemical mechanisms in combustion.

Flat flame burners are also suitable for the production of cool flames of hydrocarbons. Ballinger et al. (2007) studied the isolated stable cool flames of n-butane, n-pentane, n-heptane, various primary reference fuels and di-t-butyl peroxide.

2.2 Octane Number Research

In the modern processes for the manufacture of gasoline, proper control of the operation requires the use of rapid methods of octane number (ON) determination. From all the works reviewed above that used a flat flame burner for various purposes, there were very few that tried to correlate the flame characteristics of a fuel to its ignition properties. However, there have been many other works that have studied combustion

parameters and their relation to octane number of a fuel. This section presents an overview of some works that focused on octane number studies.

The experimental study performed by Stepanski et al. (1986) aimed on producing a detailed analysis of the correlation between ON and the parameters of the process of mild (cold flame) oxidation of gasoline in a flow reactor. The experimental data indicated that the correlation between fuel ON and the coordinate maximum temperature is very clear cut under the following process condition: air feed rate 1.46 liters/min, fuel feed rate 0.026 liter/min and temperature 345 C. Experiments were performed under these conditions, using model mixtures consisting of n-heptane and iso-octane, and also on commercially produced naphthas. The relationship between the coordinate of the maximum temperature and the fuel ON made by Stepanski et al. (1986) is shown in Figure 2.4. Their results indicated that the correlation found between ON and the characteristics of the fuel oxidation process in a flow reactor can be used as the basis for a routine control method of octane number determination.

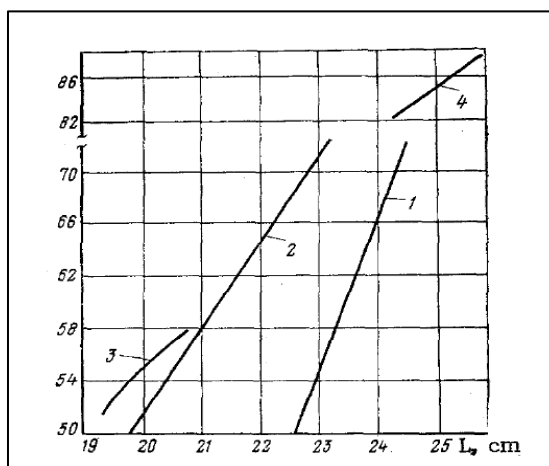


Figure 2.4: Position of temperature max along reactor length L as a function of ON 1) model mixture; 2) model mixture, differential thermocouple; 3) straight-run naphtha; 4) naphtha frp

Source: Stepanskii et al. "Correlation between octane number and certain parameters", Chemistry and technology of fuels and oils, 1980, Vol. 16, Number 8, pp. 554-557

Apart from experimental studies, researches have also developed some mathematical models for octane number determination. Instead of using traditional PRF models to simulate RON and MON of a fuel, Morgan et al. (2010) made use of surrogate fuels for purpose of mapping gasoline compositions into RON/MON space. They primarily made use of the toluene reference fuels (TRFs) – ternary mixtures of toluene, n-heptane and i-octane and employed a 2nd order polynomial to map these compositions into RON and MON based on new experimental data for the octane numbers of these toluene reference fuels. This mapping was then inverted, allowing one to calculate the composition of surrogate blend according to the specified RON and MON of a real fuel. This study enables one to use two simple formulae to determine, for a given fuel with known RON and MON, the volume fractions of toluene, n-heptane and iso-octane to be blended in order to emulate that fuel.

$$p = \frac{RON - (a_{tol}x_{tol} + a_{tol^2}x_{tol}^2)}{100 + a_{tol,p}x_{tol}}$$

$$\begin{aligned} \text{Sensitivity (RON - MON)} &= \\ &= a_{S,tol}x_{tol} + a_{S,tol^2}x_{tol}^2 + \frac{a_{S,tol}x_{tol}(RON - (a_{R,tol}x_{tol} + a_{R,tol^2}x_{tol}^2))}{100 + a_{R,tol,p}x_{tol}} \end{aligned}$$

where, p is a renormalization of PRF, a's represent the coefficients of toluene (tol), iso-octane and n-heptane, x is the volume fraction and subscript R, S refer to RON and sensitivity coefficients.

2.3 Quenching Research

Most research performed in this area relates to stretching and straining of premixed flames. Information on the quenching of turbulent flames at high pressure is important for the design of practical combustors and for improved fundamental understanding of turbulent combustion. The increased flame stretch rate arising from turbulence narrows the bounds for turbulent combustion. Experimental studies of turbulent premixed flame quenching have covered variety of mixtures and pressures. Abdel-Gayed et al. (1987) performed experimental studies on the topic and collated his findings in terms of the Karlovitz stretch factor, K , and Lewis number, Le , for flame. Meneveau et al. (1991) performed direct numerical simulations of quenching and were in agreement with experimental findings. They assumed that the quenched parts of the flame had no influence upon the active parts. In the quenched parts burned gas was penetrated by reactants and cooled by them. This cooling might be sufficient to induce localized quenching, but this was difficult to quantify. Yang et al. (2002) studied the effects of radiative heat loss from CH_4 -air flames at atmospheric pressures using a cruciform burner. Critical values of K for global quenching were found, with control of radiative loss by N_2 and CO_2 dilution. This was further studied by Bradley et al. (2007) at wide range of pressures and with more compositions. Bradley et al. (2007) carried out experimental and theoretical studies on turbulent flame quenching with premixed flames of methane-air, iso-octane-air and hydrogen air. They explored the influences of laminar flame extinction stretch rates and high pressure on turbulent flame quenching. A variety of mixtures were exploded in fan-stirred explosion bomb, up to the point of flame extinction. Only the very rich iso-octane-air mixtures that produced sooting flames and near-limit H_2 -air flames were radiative losses significant. The compositional changes principally affected the laminar burning velocity, u_i , extinction rate, and Ma_{sr} , Markstein number which is considered as a more fundamental parameter for strain rate. They found

that the ratio of the positive stretch rate for extinction of the laminar flame to the root mean square turbulent strain rate was an important parameter.

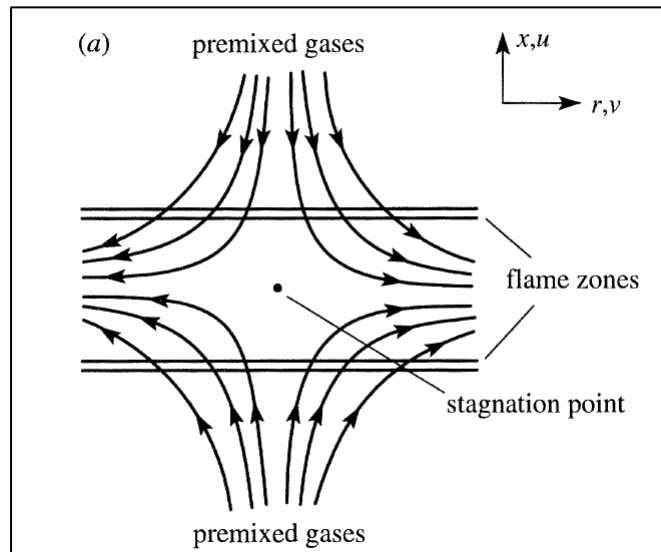


Figure 2.5: Unburnt-to-unburnt opposed flow, premixed flame configuration

Source: Graham Dixon-Lewis, "Laminar premixed flame extinction limits I- Combined effects of stretch and upstream heat loss in the twin-flame unburnt-unburnt opposed flow configuration", *Mathematical, Physical and Engineering Sciences*, Vol. 452, No, 1951 (August 1996)

Opposed flow configuration forms a popular method for flame extinction studies. Dixon-Lewis (1996) employed a symmetric unburnt-to-unburnt opposed flow configuration, as shown in Figure 2.5, to examine the combined effects of stretch and localized upstream heat loss on the properties of a stoichiometric laminar premixed methane-air flame. In an unburnt-to-unburnt opposed flow, fresh combustible mixture of fixed composition inside the flammability limits is discharged towards the stagnation plane from two identical coaxial nozzles maintained at constant temperature, and separated by a fixed distance. In this case, a sufficient increase of the input velocity, with its accompanying increase of strain rates throughout the system, will produce an abrupt,

real extinction limit. Such limits have been observed experimentally, for essentially adiabatic near-stoichiometric flames, by Sato (1983), Law et al. (1987) and others.

Experiments in motored engines and rapid compression machines show that under typical engine conditions the auto-ignition of the fuel is a two-stage process and it is clear that a logical approach to the problem of knock in gasoline engines requires a quantitative understanding of two-stage ignition and the closely related phenomenon of cool flame periodicity. In the study performed by Halstead et al. (1971), two stage ignition of cool flame oxidation of acetaldehyde was discussed. From the results, it can be deduced that there is a chemical run away condition that is followed by a thermal run away condition. The shield gas in this experiment changes the thermal run away condition. Thermal runaway occurs when the reaction rate increases due to an increase in temperature, causing a further increase in temperature and hence a further increase in the reaction rate. Thermal runaway can occur because, as the temperature increases, the rate at which heat is removed increases linearly but the rate at which heat is produced increases exponentially. The shield gas acts as a chemical that cancels the effect of the catalyst that causes the thermal run away condition. Therefore, the nitrogen or helium act as quenching agents and provide a medium for heat loss from the flame.

CHAPTER 3: EXPERIMENTAL MODEL AND PROCEDURE

3.1 Experimental Configuration

The study focused on conducting premixed combustion experiments with primary reference fuel (PRF) which is a mixture of iso-octane and n-heptane to determine the octane rating of commercial gasoline. Different volume mixtures of PRF fuel were studied and were distinguished by their quenching results. Different octane number fuels showed different behavior when under quenching tests. Fuels that were used for experiments were PRF 0 (n-heptane), PRF 100 (iso-octane), PRF 65 (65% iso-octane, 35% n-heptane) and PRF 85 (85% iso-octane, 15% n-heptane). At first, premixed flames for n-heptane and iso-octane were studied for different equivalent ratios or air-fuel ratios. It is important to define and differentiate between an air fuel ratio and equivalence ratio. Air-fuel ratio is the mass ratio of air to fuel present during combustion. If exactly enough air is provided to completely burn all of the fuel, the ratio is known as stoichiometric ratio. Mixtures below the stoichiometric ratio with more air are called lean and mixtures above the stoichiometric with more fuel are called rich mixtures. In order to neglect the units being used, the term equivalence ratio is used over fuel-to-oxidizer ratio. Equivalence ratio of the system is defined as the ratio of the fuel-to-oxidizer ratio to the stoichiometric fuel-to-oxidizer ratio.

$$\phi = \frac{\text{fuel-to-oxidizer ratio}}{(\text{fuel-to-oxidizer ratio})_{st}} = \frac{m_{\text{fuel}}/m_{\text{ox}}}{(m_{\text{fuel}}/m_{\text{ox}})_{st}} = \frac{n_{\text{fuel}}/n_{\text{ox}}}{(n_{\text{fuel}}/n_{\text{ox}})_{st}}$$

where m is the mass, n is the number of moles, and st stands for stoichiometric.

Flat flames have been used as a laboratory flame to study the ignition of fuel mixtures with single-and two-stage phenomena. A flat flame test rig was established for this study. The flat flame burner that was used to study quenching of premixed flames is

known as the McKenna Flat Flame Burner and is supplied by Holthuis & Associates (Sebastopol, CA). This Flat-Flame Burner is constructed of stainless steel housing within a main-body. Pressed into the housing is a fluid cooled 6 cm diameter burner plug made up of sintered stainless steel. The housing unit is then screwed into the main body and a flanged mounted sintered porous bronze shroud ring is fixed over the housing onto the main body. The fuel mixture consisting of premixed oxidizer and fuel is introduced through an O-compression fitting into the bottom of the housing and distributed evenly through the sintered matrix plug cross section. Any pressure surge in the fuel flow is normalized in the cavity located below the sintered plug within the housing. Likewise the concentric shroud ring inert gas O-compression fitting into the main body insures a dampened smooth flowing shielding of the flame from the outside environment and stabilizes the flame above the sintered plug. A cooling circuit within the plug matrix is embedded during the sintering process. It consists of an equally spaced helix of 1/8 inch metal tubing planar to the plug surface, thereby any radial temperature gradient is minimized. The cooling of the plug further prevents flash back from occurring. The porous ring surrounding the central region is used for nitrogen gas flow in order to isolate the flame from the ambient disturbances. A labeled diagram of the McKenna flat flame burner is shown in Figure 3.1.

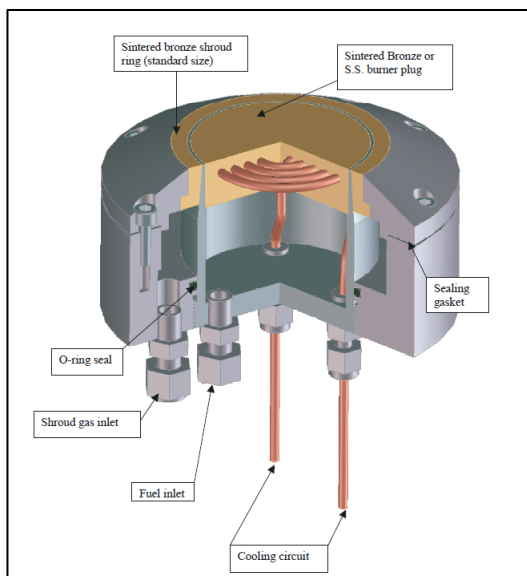


Figure 3.1: McKenna Flat flame burner

Source: Holthuis & Associates, Mckenna Flat Flame Burner manufacturer, Sebastopol, CA

After several tests performed on the burner at high temperatures, the central sintered plug was damaged. The extreme temperatures of the flames made it expand and extend upwards from the burner surface. Hence, the replacement was made with tapered edges inside to ensure the sintered plug to remain fixed at its place as it posed a safety hazard. Therefore, the burner design that produced all the results in this study had a unique design with tapered edges to prevent damage. The dimensions including diameter of the central core, shroud ring and height of this burner are given in Figure 3.2.

Other major components of the test rig include a 750 W cartridge heater as the fuel vaporizer, a Gilson HPLC piston pump (Mole 305 with 100 SC pump head) used to set the liquid fuel flowrate, an Aalborg Mass flow meter to regulate the air flowrate, temperature controlled heating tape to increase the temperature of premixed fuel air mixture, a thermistor, thermocouples for temperature measurements, personal computer and Data Acquisition for recording temperature and finally stainless steel and Tygon

tubing. Table 3.1 shows the list of equipment with model information. The test rig arrangement is illustrated in Figure 3.3.

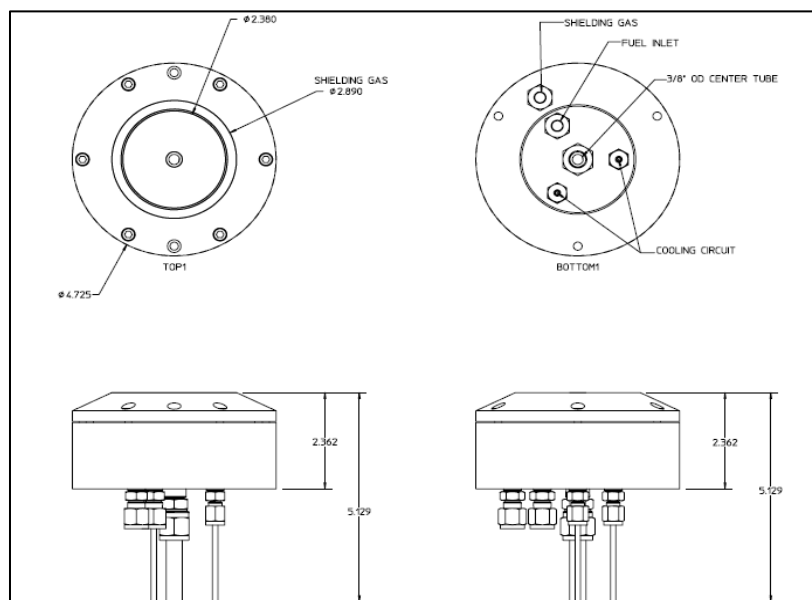


Figure 3.2: Dimensions of McKenna Flat flame burner

Source: Holthuis & Associates, Mckenna Flat Flame Burner manufacturer, Sebastopol, CA

Table 3.1: Test equipment list with description

#	Equipment name	Description
1	Mckenna Flat Flame Burner	Stainless steel burner plug with tapered edges from Holthuis & Associates
2	Air mass flow meter	AALBORG GFM 47-Air, Range 0 – 100 l/min
3	Nitrogen rotameter	Matheson Tri-gas, Model # FM-1050
4	Ignitor	Propane fuel cylinder
5	Fuel pump	Gilson 305 pump
6	Cartridge heater with Variac	Variable autotransformer, SSTACO Energy products Co., Model # 3PN1010B
7	Heating tape	Brisk Heat- Heating tape with percentage control, BSAT101008

Table 3.1 - Continued

8	Thermistor	OMEGA – DP80 Series
9	Data Acquisition	LOtech Personal DAQ/3000 Series, 16-bit/1-Mhz USB DAQ system
10	Camera	EXILIM Digital camera EX-F1, 60 fps, 12x optical zoom, 36-432 mm (35 mm EQUIV)
11	Spectrometer	Oriel Corporation, Model # 77250

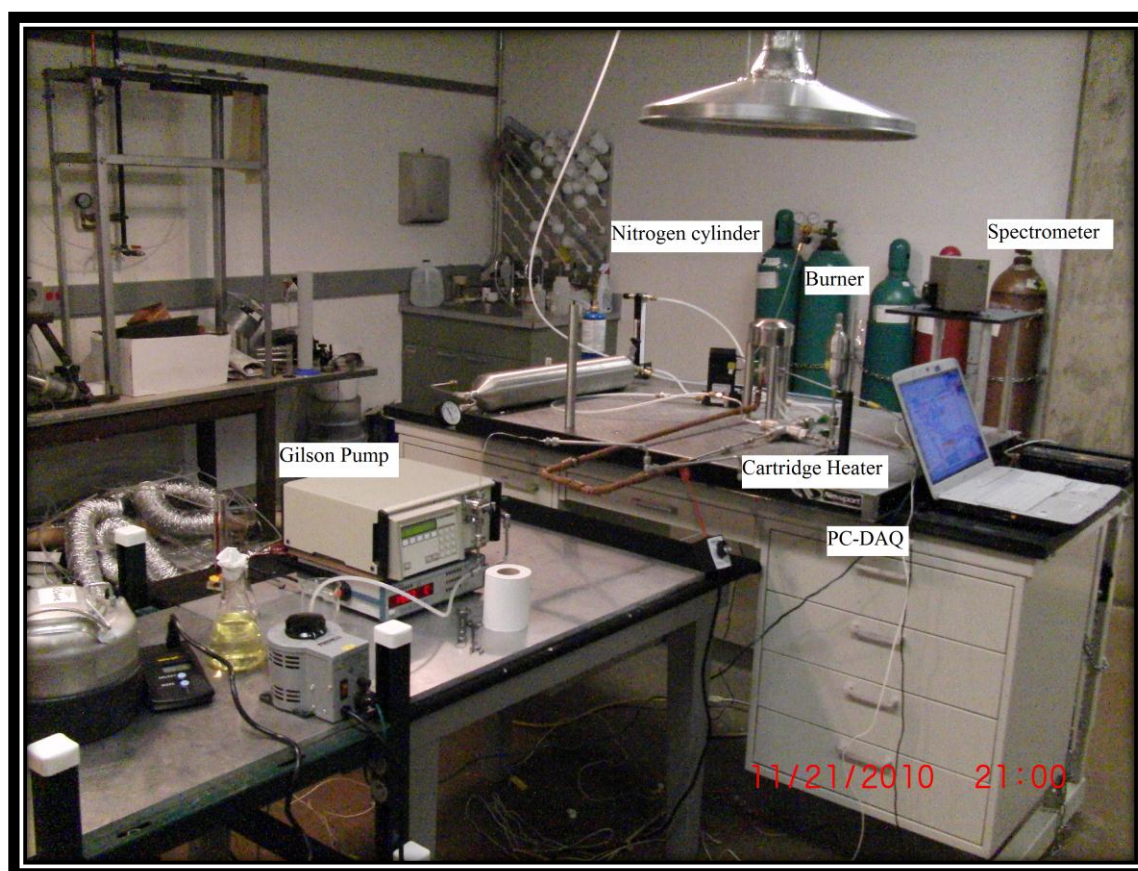


Figure 3.3: Experimental test arrangement

Liquid fuel being used is filled in the stainless steel tank with tight fitted caps. Once the Gilson pump is turned on, the fuel is pumped out of the fuel tank and is transported using stainless steel tubing. The cartridge heater running at very high

temperatures (400-450 C) then vaporizes the liquid fuel and is mixed with the incoming air at the four-way cross. The four-way cross consists of air and fuel inlet, third side for the cartridge heater and fourth side for the fuel air mixture outlet. Fuel air mixture is then transported through the tubing while it is heated up using an external heating tape to the desired temperature before it enters the burner. The desired temperature of the fuel air mixture at the inlet of the burner is about 180 C (453 K). The mixture is then ignited using an external torch above the burner. The temperature is measured at two locations. First at the cartridge heater to make sure the all of the liquid fuel is being vaporized and second, at the inlet of the flat flame burner. A cylindrical tank is used as a capacitor to provide stability to the incoming airflow which sits upstream of the air flow meter. Two K-type thermocouples are used for the setup. First thermocouple connected to the cartridge heater has its display on the thermistor and the second thermocouple fixed at the burner inlet is connected to the computer with the help of a DAQ. Cooling water pipes run from regular tap water source through the burner water circuit when under operation to prevent overheating of the burner.

Apart from the basic test setup, a spectrometer and camera are used for taking flame images. A spectrometer is an instrument that is used to measure properties of light over a specific spectrum. The variable measured is most often the flame's intensity, but in this case is to visualize lift-off. The independent variable is the wavelength of the flame. Gas tanks of nitrogen (N_2) and helium (He) are used primarily for the secondary gas flow that helps in flame entrapment and lift-off. This will be discussed in detail in the results section.

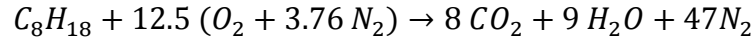
3.2 Methodology

Prior to conducting the combustion experiments with flammable fuels, it is necessary to carry out all the governing calculations in order to conform to safety. The principal calculations in this study related to the mass flow rate, temperature and heat requirement calculations. Calculation spreadsheets were made for PRF 0, 65, 85, 100 and PRF toluene. General methodology for the calculations for PRF 100 (iso-octane) is presented in this section and was basically reused for other mixtures by changing their properties. At first the volumetric flow rate was calculated by assuming the flashback velocity of the fuel air mixture to be 0.5 m/s. The temperature of mixture entering the burner was maintained at 180 C (453 K). The following table shows the primary calculations that are discussed in detail in this section.

Table 3.2: Input calculations for iso-octane

d (in)	2.38	$\rho_{\text{air}} (453\text{K}) [\text{kg}/\text{m}^3]$	0.78
T (K)	453	$\rho_{\text{air}} (20\text{C}) [\text{kg}/\text{m}^3]$	1.18
Diameter (m)	0.06	$\rho_{\text{io}} (453\text{K}) [\text{kg}/\text{m}^3]$	3.07
Velocity (Flashback) (m/s)	0.5	$\rho_{\text{liq_io}} (20\text{C}) [\text{kg}/\text{m}^3]$	700
Volume flow rate (m^3/s)	1.44E-03	Input iso-octane flowrate [ml/min]	6.25
M -air (g/mol)	28.97	Input air flowrate [l/min]	55.74
M -iso-octane (g/mol)	114.23		
ER	1		
$n_F/n_{A,st}$	1.68E-02	Air + Fuel mixture flow rate [m^3/s]	1.44E-03
n_F/n_A	1.68E-02	Area out [m^2]	2.87E-03
Air volumetric flow (m^3/s)	1.41E-03	Exit Velocity [m/s]	0.33
Air mass flow (kg/s)	1.10E-03	Area of nitrogen shield [m^2]	1.36E-03
Air volumetric flow (m^3/s), stp	9.29E-04	Nitrogen Flow rate [l/min]	27.12
Air mass flow, 20 C (l/min))	5.57E+01		

Before calculating the mass flow rates of fuel and air separately, the stoichiometry of the chemical equation is determined. Following is a balanced combustion equation for iso-octane.



Now, at stoichiometric condition, fuel-air ratio is calculated as follows:-

$$\frac{n_f}{n_A}, st = \frac{1}{[12.5 \times (3.76 + 1)]} = 1.68 \times 10^{-2}$$

The actual fuel air ratio is just calculated by,

$$\frac{n_f}{n_A} = \frac{n_f}{n_A}, st \times \phi$$

where, subscript st stands for stoichiometric, and ϕ is the equivalence ratio (ER).

Next, the volumetric flow rate of air and fuel can be calculated in m^3/s .

$$\dot{Q}_a = Q \times \frac{1}{(1 + \frac{n_f}{n_A})}$$

$$\dot{Q}_f = Q \times \frac{(\frac{n_f}{n_A})}{(1 + \frac{n_f}{n_A})}$$

Densities for iso-octane at liquid and vapor state are calculated using the ideal gas law and are displayed in the table.

$$P = \rho RT$$

Using the densities, the mass flow rate of fuel and air is calculated in l/min.

$$\dot{m} = \rho Q$$

Once the fuel air mixture flow rate is known, it is required to calculate the required flowrate for the secondary gas flow. Using continuity equation and keeping velocity constant, the flowrate for secondary gas flow rate is calculated.

$$Q_{mix} = Q_a + Q_f$$

$$Q = V A$$

Using the exit velocity of fuel air mixture, and with a given shroud area, flow rate can be calculated. All the flow rates are converted into liters/minute to be in accordance with the mass flow meters used for fuel and air. The results in the table show the input flow rates of iso-octane and air at equivalence ratio of 1.0. Similar calculations were done for n-heptane, PRF mixtures of 65 and 85 and toluene. Following is presented safety guidelines prepared for experimental testing and the outline procedure.

3.2.1: Safety Procedure

Start Up Procedure:

1. Inspect lab area for possible safety hazards.
2. Put on necessary safety equipment (goggles, gloves, lab coats, etc).
3. Make sure that the fire extinguisher is in place.
4. Turn on power for power switch.
5. Turn on computer.
6. Open air valve and adjust to appropriate flow rate and let it run for about 3 minutes.
7. Turn on heating tape to 100%.
8. Turn on Variac to 40% (this can be adjusted later, but to get things warm, 40% is appropriate).
9. Monitor the thermocouple temperature using the Omega Analog Indicator.
10. Turn on the Ignitor.
11. Put Gilson pump feed into fuel. Adjust fuel flow rate as needed, but do NOT begin pumping.
12. When thermocouple reaches appropriate temperature, begin Gilson pump.

Shut Down Procedure:

1. Switch the valve on the Gilson pump to force water to remove fuel. Run for 2-3 minutes with water then stop the pump and turn it off.
2. Shut off Variac.
3. Shut off heating tape.
4. Remove fuel feed from fuel.
5. Store fuel in appropriate location in the fire cabinets.
6. When computer/thermocouple indicates that temperatures have dropped below 125°C, run the air through the burner for about 5 more minutes to ensure there is no remaining fuel or liquid in the system.
7. Shut off the air flow.
8. Turn off computer if not needed any more.
9. Turn off power strip.
10. Return safety equipment to appropriate location.
11. Perform final safety check to ensure everything is put away and stored properly.

Emergency Procedures

1. Small fire (about 1 cubic foot):
 - If you know what is burning, use the designated fire extinguisher.
 - If you don't know, then call the fire department. Inform UI Public Safety and Facilities Management.
2. Large fire:
 - Leave the room immediately and confine the fire by closing doors.
 - Activate the nearest fire alarm.
 - Dial 911, alert others and assemble at a safe location, wait for fire department to arrive.
3. Liquid spill:
 - If you get liquid on your face or eyes, wash thoroughly at the eye wash station.

- Do not plug or unplug any electrical equipment.
- Inform others about the spill and report it to the supervisor.

3.2.2: Experimental Procedure

1. Fuel to be used is prepared and filled in to the fuel tanks.
2. Air supply along with cooling water is turned on.
3. Cartridge heater is turned on and set to about 40% and above 400 C and heating tape is turned on and temperature at the inlet of burner is brought to 180 C which is observed using a computer connected to a DAQ and a thermocouple.
4. Gilson pump is turned on and the required flowrate is set.
5. Once the desired temperature is reached, the pump is started and a torch is used to light the fuel air mixture at the burner exit.
6. Next the secondary gas tank (N₂, He) is turned on and set to required flow rate to match equal exit velocity of fuel air mixture.
7. Camera is mounted on a stand at the flame height and is operated with dimmed lighting.
8. Spectrometer is also seated on stand and is adjusted so the lens on the spectrometer covers the full flame length.
9. The dial on the spectrometer is turned in increments of 25 nm to get images of the flame at different wavelengths that are captured using the camera

3.3 Assistive Computational Study

3.3.1: FLUENT

Besides the ongoing experimental study of the quenching phenomenon on premixed flames, a computational study was performed to gain insight into the mixing between the fuel-air mixture and the shielding nitrogen gas, and to aid determination of test conditions. A 3-D model of the flat flame burner was created and analyzed. Using the dimensions of the burner core and the shroud area, a 3-D mesh was created in Gambit.

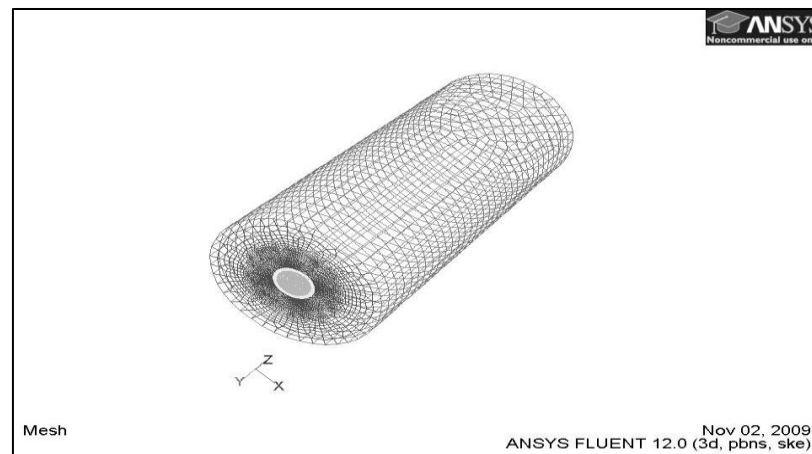


Figure 3.4: 3D mesh of burner model

The geometry consisted of burner core and the shroud as a circular surface surrounded by larger circle with four times the diameter of the burner. The surrounding circular surface was then extruded to form a cylindrical shape to model the surrounding ambient effects. The height of the cylinder was made to be ten times the diameter which is equivalent to the exhaust present above the burner. The mesh was created much finer on the burner core surface, its shroud and also in the surrounding base. The surfaces far away from the burner were given a coarser mesh as the computations near the base were more important. The fuel air inlet zone (burner core), the nitrogen shroud zone and the

surrounding zone were all given the velocity inlet boundary conditions with a velocity of 0.5 m/s for the fuel-air mixture as well as the co-flowing nitrogen, and 0.05 m/s for the ambient air. The surface opposite the burner was made the exhaust and the cylinder wall was just treated as a wall boundary condition. This mesh was then exported to FLUENT and was analyzed using k-e turbulence (non-adiabatic) and combustion species model. The temperature at the fuel-air inlet zone was set to be 2000 K in order to ignite the mixture. Fuel-air mixture jet was set to be 453 K with nitrogen gas and surrounding air at room temperature, 300 K. Temperature contours were projected on a perpendicular z-plane and plumes of decreasing temperatures were seen.

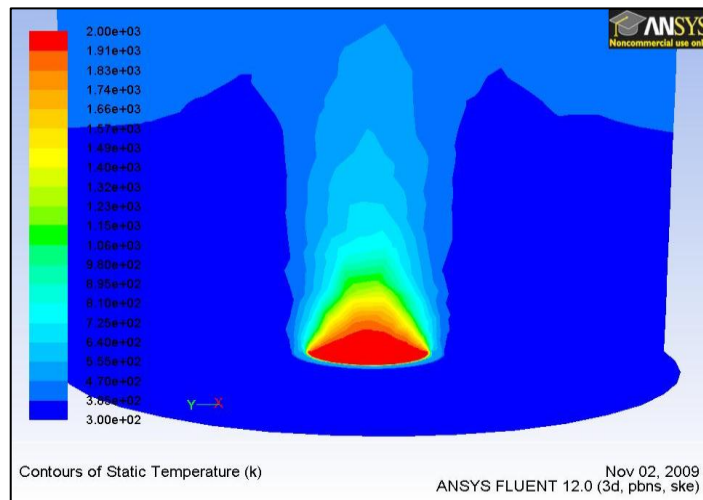


Figure 3.5: Temperature contours projected on plane perpendicular to burner base

The goal of this computational study was to understand the interaction of nitrogen gas particles at room temperature with the hot flame. Consequently, the velocity vectors were plotted to see the movement of the gas streams.

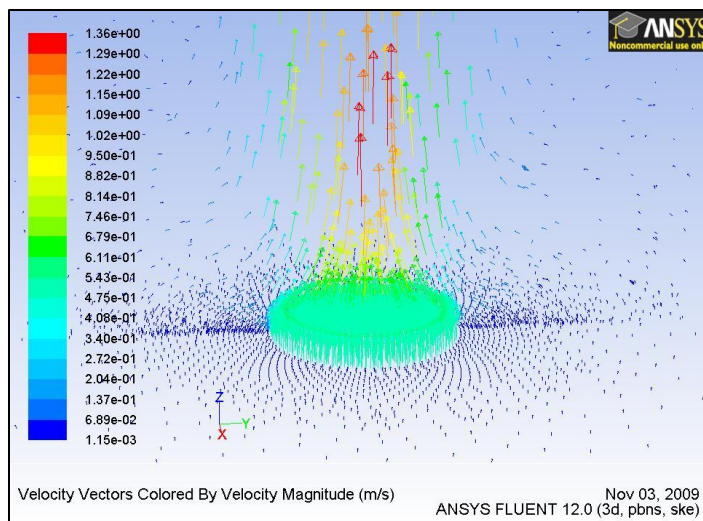


Figure 3.6: Velocity vectors of flame, nitrogen and surrounding air

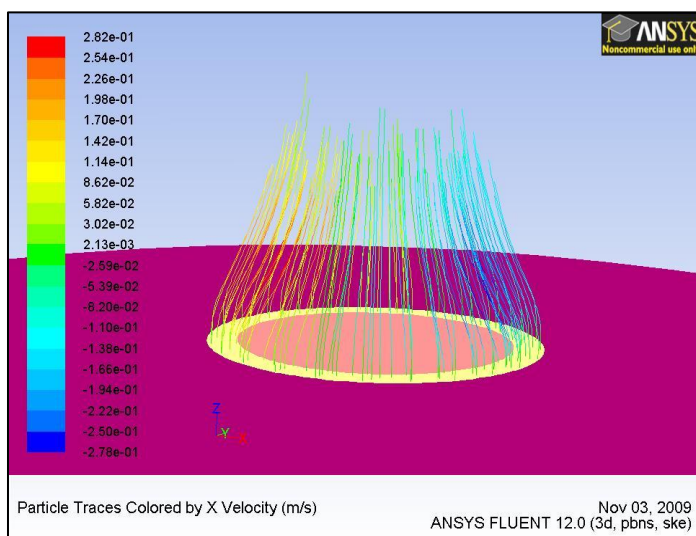


Figure 3.7: Particle traces colored by x-component velocity (m/s)

It was seen that nitrogen gas velocity vectors could shield the inner hot flame up to certain height after which the surrounding air would envelop the flame. The velocity also increased towards the center which was due to the isotropic thermal expansion and upward buoyant acceleration. The distance up till which the nitrogen gas was able to

shield or quench the flame was approximated to be about 50 mm or 1.97 inches which was later verified with the experimental study.

When the x-component velocities of the nitrogen gas were plotted that is directed towards the center of the burner. It was noted that the nitrogen particles showed the tendency of moving towards the center of the flame thus explaining the lift off phenomenon. The lift off of the flames is presented in the experimental results section.

3.3.2: CHEMKIN

CHEMKIN is a chemical kinetics software program that contains an extensive library of reactor models, including batch, continuous-stirred, and plug flow reactors. The software has the capacity to solve rigorous kinetics models consisting of multiple reactors interacting with each other. The CHEMKIN interface contains a diagram view in which blocks representing different reactors are laid out on a workspace, and connections between the blocks represent reactant and product flow streams. After the setting up the reactor flowsheet, the chemistry set must be pre-processed before the model can be run. Pre-processing is also required before any further model input is entered. A chemistry set consists of input files that contain species and reaction parameters, as well as thermodynamic data and gas transport property data. When the pre-processor is run, these files are verified for consistency and completeness. After the appropriate mechanism is specified, the CHEMKIN software utilizes several conservation equations to iteratively model chemical reaction kinetics

The PREMIX model was selected for this study that predicts the structure of steady laminar, 1-D premixed flames. This model is capable of predicting temperature and species profiles in two laminar premixed flame configurations. The first is the burner-stabilized flame with a known mass flow rate. This configuration can be run in two different cases, one where the temperature profile is known and one in which the

temperature profile is determined by the energy conservation equation. As it was difficult to obtain an accurate temperature profile from the experiment, the program was made to use a burner stabilized flame model in which the temperatures are determined from solving the energy conservation equation.

The governing equations that are used by the PREMIX model to solve for temperature and species profiles for steady, isobaric, quasi-one-dimensional flame propagation are as follows:

Continuity:
$$\dot{M} = \rho u A$$

Energy:
$$\dot{M} \frac{dT}{dx} - \frac{1}{c_p} \frac{d}{dx} \left(\lambda A \frac{dT}{dx} \right) + \frac{A}{c_p} \sum_{k=1}^K \rho Y_k V_k c_{pk} \frac{dT}{dx} + \frac{A}{c_p} \sum_{k=1}^K \dot{\omega}_k h_k W_k = 0$$

Species:
$$\dot{M} \frac{dY_k}{dx} + \frac{d}{dx} (\rho A Y_k V_k) - A \dot{\omega}_k W_k = 0$$

Equation of State:
$$\rho = \frac{p \bar{W}}{RT}$$

In these equations x denotes the spatial coordinate; \dot{M} the mass flow rate (which is independent of x); T the temperature; Y_k the mass fraction of the k th species (there are K species); p the pressure; u the velocity of the fluid mixture; ρ the mass density; W_k the molecular weight of the k th species; \bar{W} the mean molecular weight of the mixture; R the universal gas constant; λ the thermal conductivity of the mixture; c_p the constant-pressure heat capacity of the mixture; c_{pk} the constant pressure heat capacity of the k th species; $\dot{\omega}_k$ the molar rate of production by chemical reaction of the k th species per unit volume; h_k the specific enthalpy of the k th species; V_k the diffusion velocity of the k th species; and A the cross-sectional area of the stream tube encompassing the flame (normally increasing due to thermal expansion).

The mechanisms that were tried to model kinetic sets of PRF mixtures were detailed chemistry sets from LLNL (Lawrence Livermore National Laboratory) and Pitsch. But the LLNL mechanism did not consist of a transport property file and hence Pitsch mechanism for PRF mixtures was used. After the chemistry sets were pre-processed, the reactor physical properties, grid properties, intermediate species and product species were entered. Next the stream properties were required that included the inlet velocity of the mixture and following the species properties such as the equivalence ratio, fuel and oxidizer fractions and combustion products. The solutions were analyzed by producing temperature and species profile plots versus the distance above burner. Due to the large size of species and reactions present in the chemistry sets of PRF mixtures, the software required enormous memory space for the simulation. The limitation of available memory space produced a grid dependent solution.

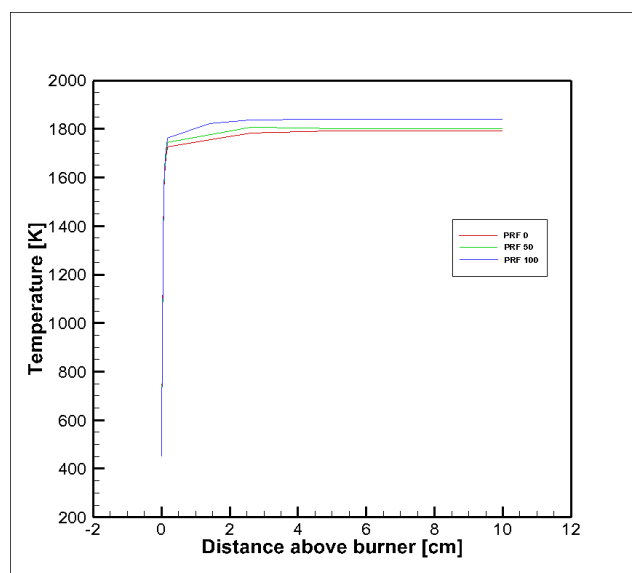


Figure 3.8: Temperature profiles as a function of distance above burner for PRF 0, 50 and 100 at ER =1.0 with 122 grid point solution

The temperatures increased with increase in octane number of the PRF fuels. From previous studies it was determined that at certain equivalence ratios, species like OH and HCO could be used to determine the difference in auto-ignition characteristic of fuels. Therefore, the species profiles were also plotted with respect to the distance above the burner.

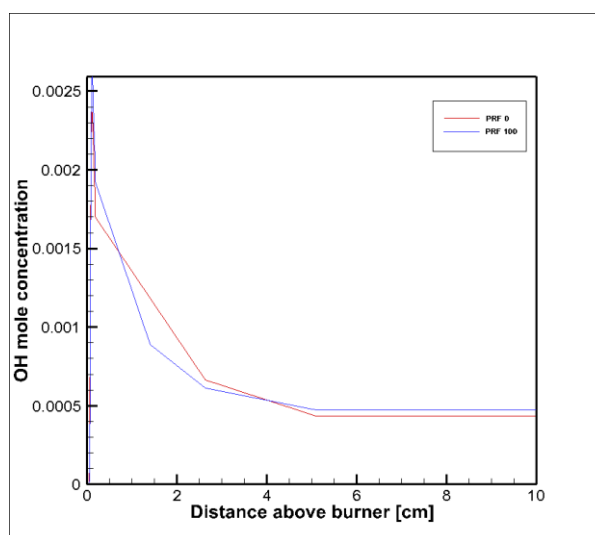


Figure 3.9: OH mole concentrations as a function of distance above burner for PRF 0 and 100 at ER = 1.0 with 122 grid point solution

The highest grid point solution that could be achieved contained 122 grid points that was run on a machine with 16 GB RAM. However, a completed solution couldn't be achieved due to computational memory constraint. As a reason for not being able to produce a higher grid point solution, the results obtained from CHEMKIN to show differences in different PRF fuels could not be confirmed or validated. Due to the above stated reasons, it was decided to use comparatively less extensive mechanisms to study combustion characteristics.

In an internal combustion engine, the flame speed of a fuel is a property which determines its ability to undergo controlled combustion without detonation. Flame speed is used along with adiabatic flame temperature to help determine the engine's efficiency. Studies performed on estimating laminar burning velocities provide great interest for the development of combustion models that provide significant information to be used as a tool for the optimization and design of specific internal combustion engines. The laminar burning velocity is an important parameter of a combustible mixture, as it contains fundamental information of reactivity, diffusivity, and exothermicity. The value of the flame speed has important effects upon the propensity of the flame to flashback and blowoff, and it also controls other key combustion characteristics, such as the flame's spatial distribution.

In recent years, biomass energy has received a lot of attention and on the contrary very few researches have been performed to study the combustion properties of biomass derived flames. Realizing the importance of developing a stronger understanding of laminar burning velocities and adiabatic flame temperatures and also the growing importance of biomass flames, it was decided to carry out a computational study using the gained knowledge of CHEMKIN to model laminar burning velocities and temperature profiles for biomass derived flames such as Syngas, landfill gas and gasification gas. The GRI-Mechanism was employed for this purpose. GRI-Mech 3.0 is a widely-used mechanism designed to model natural gas combustion. It contains 325 elementary chemical reactions and thermochemical parameters for the 53 species involved. The set is optimized for pressures up to 10 atm and equivalence ratios between 0.1 and 5.0.

The second flame configuration of the PREMIX model was used to study laminar burning velocities of biomass derived flames, which is called the freely propagating adiabatic flame model. In this model, there are no heat losses and thus temperatures are computed from the energy equation. It is capable of calculating flame speeds by

predicting the temperature distribution that is important for flammability studies. The model solves for the mass burning rate as per the following relation, which is the eigenvalue of the problem, and thereby calculate the flame speed from the known unburned density.

$$\dot{m} = \rho_u S_L$$

where, \dot{m} is the burning rate, ρ_u the unburned density and S_L laminar burning velocity.

The input parameters that were used to construct the model are given in Table.

Table 3.3: Input parameters for PREMIX Flame model

Unburnt gas temperature	300 K
Pressure	1 atm
Inlet mass flow rate	0.04 g/cm ² s
Fuel mixtures	Syngas (H ₂ , CO), Landfill gas (CH ₄ , CO ₂), Gasification gas (H ₂ , CO, N ₂)
Oxidizer	Air (79% N ₂ , 21% O ₂)
ER	0-5
Complete combustion products	CO ₂ , H ₂ O, N ₂

Different compositions of syngas, landfill gas and gasification gas were executed for comparison. The following figure displays the burning velocities and adiabatic flame temperatures as a function of equivalence ratio as computed by CHEMKIN with three different compositions of syngas, 5% Hydrogen (H₂) and 95 % Carbon monoxide (CO), 50% H₂ and 50% CO, and lastly, 95% H₂ and 5% CO.

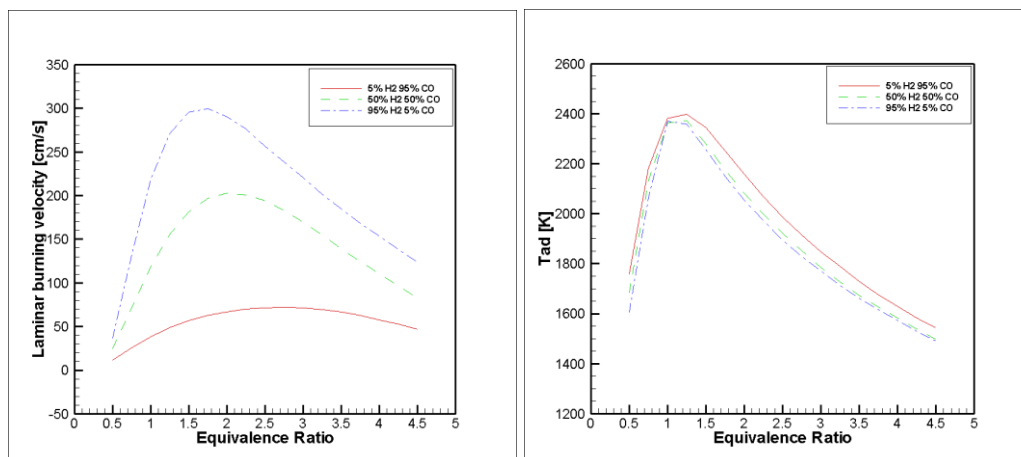
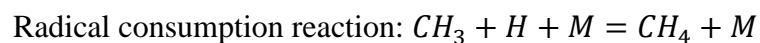
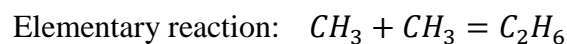


Figure 3.10: Laminar burning velocities (left) and adiabatic flame temperatures (right) versus ER for syngas compositions: 1) 5% H₂, 95% CO 2) 50% H₂, 50% CO 3) 95% H₂, 5% CO

It can be noted that the laminar burning velocities of syngas flames peak at rich mixtures. The peak shifts to the right to a higher equivalence ratio when the percentage of H₂ is decreased in the H₂-CO mixture. The burning velocities also increase with increase in percentage of H₂ in the mixture. The peak velocity with 95% H₂ and 5% CO is about 300 cm/s and drops down to about 50 cm/s with 5% H₂ and 95% CO. The maximum adiabatic temperature also occurs at rich mixtures close to an equivalence ratio of 1.3 of about 2400 K. The peak temperature decreases slightly as the H₂ percentage is increased in the mixture.

Landfill gas is a mixture of methane (CH₄) and carbon dioxide (CO₂). The compositions that were compared for landfill gas were 100% CH₄ and 0% CO₂, 90% CH₄ and 10% CO₂, and, 55% CH₄ and 45% CO₂. At lean ratios, the burning velocities decrease rapidly as equivalence ratio decreases corresponding to a rapid decrease in flame temperature. On the other hand, for the rich mixtures, the burning velocity profiles show two different regimes. In the moderate rich regime (1.00 < ER < 1.36), the burning velocity drops rapidly as equivalence ratio increases mainly due to hydrogen radical consumption. In the richer regime (ER > 1.36), there is a slower decrease of laminar

burning velocity as equivalence ratio increases due to elementary reaction being more dominant than radical consumption reaction.



The adiabatic temperature peaks at stoichiometric ratio for all compositions, but is seen to decrease with a decrease in CH_4 percentage in the mixture.

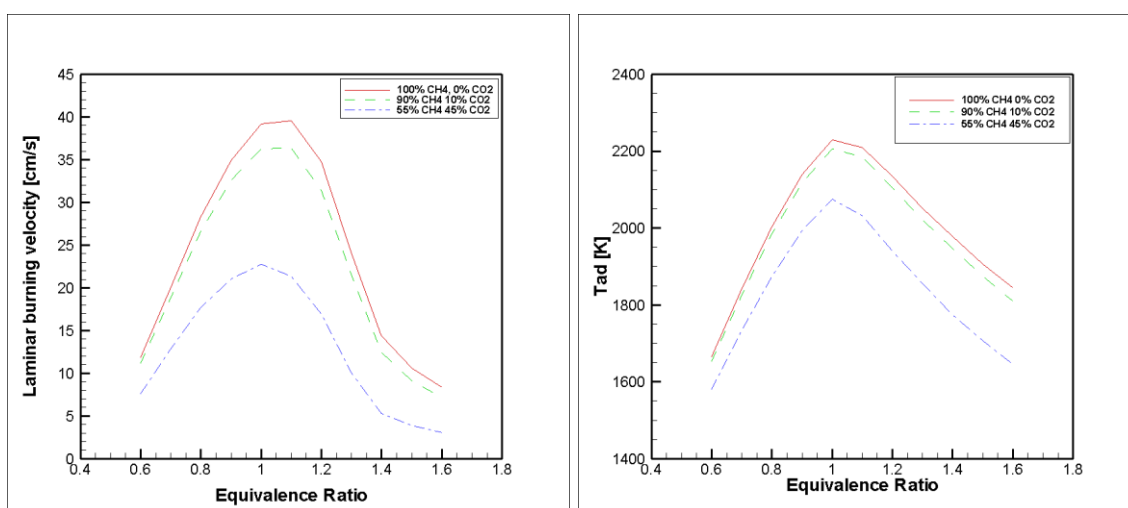


Figure 3.11: Laminar burning velocities (left) and adiabatic flame temperatures (right) versus ER for landfill gas compositions: 1) 100% CH_4 , 0% CO_2 2) 90% CH_4 , 10% CO_2 3) 55% CH_4 , 45% CO_2

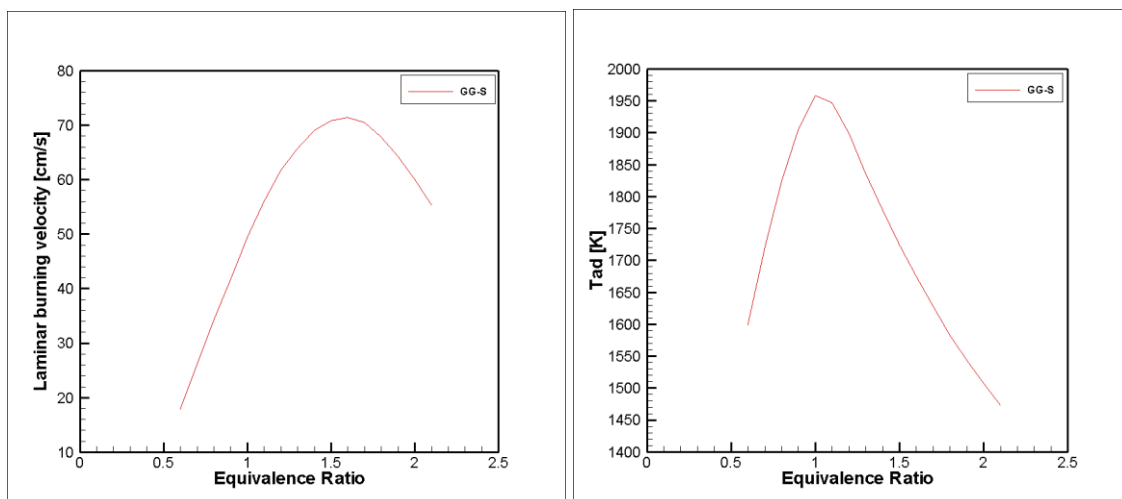


Figure 3.12: Laminar burning velocities (left) and adiabatic flame temperatures (right) versus ER for gasification gas compositions: 1) 24% CO, 21% H₂, 55% N₂

At last, burning velocities and adiabatic flame temperatures of gasification gas containing 24% CO, 21% H₂, and 55% N₂ were computed. It is seen from Figure 3.12 that the maximum burning velocity is about 0.7 m/s, that is considerably higher than the landfill gas flames, owing to the presence of hydrogen in the mixture. The laminar burning velocity peaks at equivalence ratio of about 1.6 whereas the maximum flame temperature occurs at equivalence ratio close to unity.

The CHEMKIN results were validated with the study performed by Liu et al. (2009) that studied the laminar burning velocities of biomass derived flames using GRI Mech and San Diego Mechanism in comparison to their experimental data. They studied the burning velocities, adiabatic flame temperatures, flame thickness and species profiles for various compositions of biomass derived gases.

CHAPTER 4: EXPERIMENTAL RESULTS AND DISCUSSION

The experimental results are categorized into four sections. At first, premixed flames of primary reference fuels were observed and studied. The primary aspects of the flame studied were flame intensity, color changes, flame length with respect to varying equivalence ratios for n-heptane and iso-octane. Secondly, the shroud gas was introduced and the lift-off was captured using a high definition camera for varying equivalence ratios and shroud gas velocities. The third section displays the images taken with the help of the spectrometer. The spectrometer is used to validate the lift-off seen using the naked eye and the camera and also to investigate the spontaneous emissions with respect to wavelengths. Finally, the results are quantified to show a relation between the octane number of a fuel with respect to flame quenching in the fourth section.

4.1 Flame Visualization

Flame intensity, color changes, lengths and shape were analyzed for PRF 0, 100, 80 and toluene using a high definition camera. It is empirically established that the flame color is closely related to the combustion phenomena occurring in the flame. These were studied for equivalence ratios ranging from close to stoichiometric ratio ($\phi = 1.13$), to slightly rich ($\phi=1.51$) to rich mixtures ($\phi= 1.89, 2.01$). The first set of images show the flame for n-heptane fuel (PRF 0).The fuel and air inputs are summarized in Table 4.1. The fuel flowrate was kept constant and airflow was decreased to change the fuel-to-air ratio.

Table 4.1: PRF 0 Input conditions for flame visualization

Fuel flowrate (PRF 0) [ml/min]	Air flowrate [l/min]	ER (ϕ)	Exit mixture velocity [m/s]
4.50	34.8	1.13	0.21
4.50	26.0	1.51	0.16
4.50	20.8	1.89	0.13
4.50	19.6	2.01	0.12

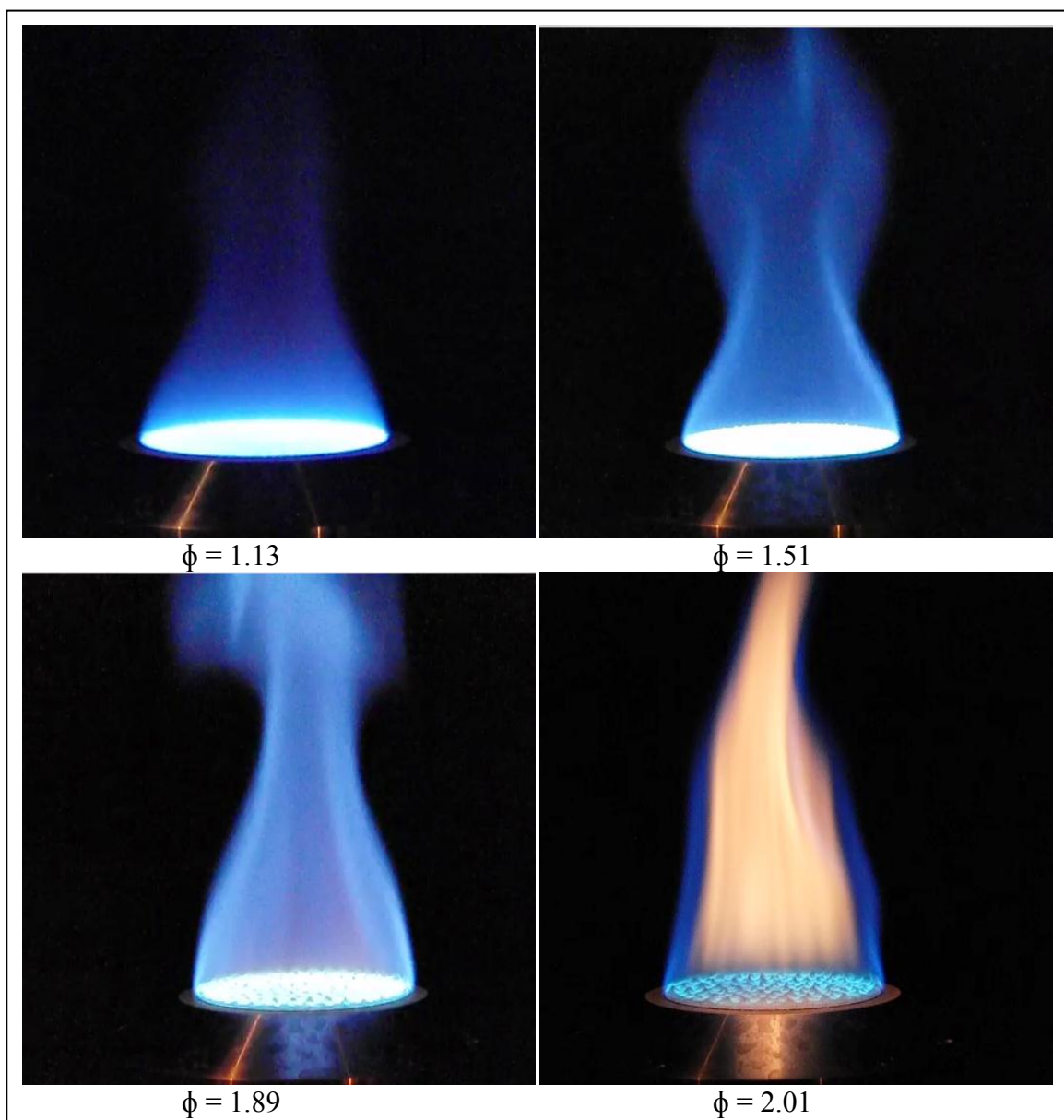


Figure 4.1: Flame images for premixed n-heptane fuel at the given equivalence ratios

The flame at equivalence ratio of 1.13 appeared short in length. Due to less amount of fuel, the color was purple or dark blue with a bright flame disc on the burner surface. The bright disc on the surface was white in color and gradually changed to a shade of darker blue going along the flame length. The bright white portion of the flame corresponds to the highest temperature zone in the flame followed by blue. The flame colors consisting of yellowish to red fall in the warmer range and are comparatively less hot. The flame for lower than equivalence ratio of 1.13 was very unstable and would extinguish itself thus making 1.13 ratio closest to stoichiometric that could be tested.

When the airflow is decreased to 26 l/min, the equivalence ratio is increased as the fuel flow is constant. The bright flame disc appears to be unchanged but the color of a nonluminous premixed flame changes from blue to blue-green as the equivalence ratio increases. This phenomenon is caused by the change of the chemiluminescence property of active molecules formed in the elementary reactions. Chemiluminescence is the emission of light with limited emission of heat as a result of a chemical reaction. The emission of light is due to the decay of the excited state to a lower level state during the reaction.

With a further decrease in the airflow, the flame moves into the richer regime with equivalence ratio 1.89. At this rich condition, the flame color changes from dark blue to light blue with a hint of orange in the middle. At this point, the bright uniform flame disc on the burner surface broke down into small cup-like structures due to the increase in instability. Flame instability is considered to consist of the combined effects: hydrodynamic instability caused by the density change across the flame and thermal-diffusive instability due to differential diffusion of reactants and energy. When premixed flame propagates outwardly, the growth rate increases and the unstable range widens caused by the combined instability between hydrodynamic and diffusion-thermal effects, which may in turn lead to the change in flame area and the consequent increase in

burning velocity. These cup-like structures get wider and bigger as the equivalence ratio increases which is due to increase in the burning velocity.

The color of the flame changes from yellow-red to yellow, depending on the temperature in the flame. This is due to the change of the thermal radiation property as the fuel to air ratio increases further. At equivalence ratio of 2.01, there is a thin film of blue flame that envelops the orange flame at the center. But as the air flow is cut down more, the blue film disappears and the flame turns to a bright orange and red.

The next set of images corresponds to the iso-octane flame. Comparisons are made with the n-heptane flame at each point. The fuel and air flowrate input table is as follows. Air flow rates were back calculated by fixing the fuel flow rate and the equivalence ratio. Due to the difference in properties of the fuels, the air flowrate and exit velocity values differ by a small amount when compared to n-heptane input table.

Table 4.2: PRF 100 Input conditions for flame visualization

Fuel flowrate (PRF 100) [ml/min]	Air flowrate [l/min]	ER (ϕ)	Exit mixture velocity [m/s]
4.50	35.5	1.13	0.21
4.50	26.5	1.51	0.16
4.50	21.2	1.89	0.13
4.50	20.0	2.01	0.12

Iso-octane flame at equivalence ratio of 1.13 appeared to be shorter in length than n-heptane but the color pattern of a bright disc at the base with purple and darker blue of the flame above remained the same. At equivalence ratio of 1.51, the flame still appeared purplish compared to n-heptane which had turned to a lighter shade of blue with lower air flow. The flame at equivalence ratio of 1.89 was similar to n-heptane but with less hint of orange. The cup-like structures formed near the base are much smaller in diameter for

iso-octane than n-heptane as the iso-octane with a higher octane number has more stability. For higher equivalence ratios, the flame appeared the same for iso-octane and n-heptane with a blue flame enveloping the orange center and finally diminishing to complete orange at extremely rich ratios. The cellular structures in the white flame disc grew larger with increase in hydrodynamic and thermal diffusive instabilities. Figure 4.2 shows the flame images for iso-octane taken at various equivalence ratios.

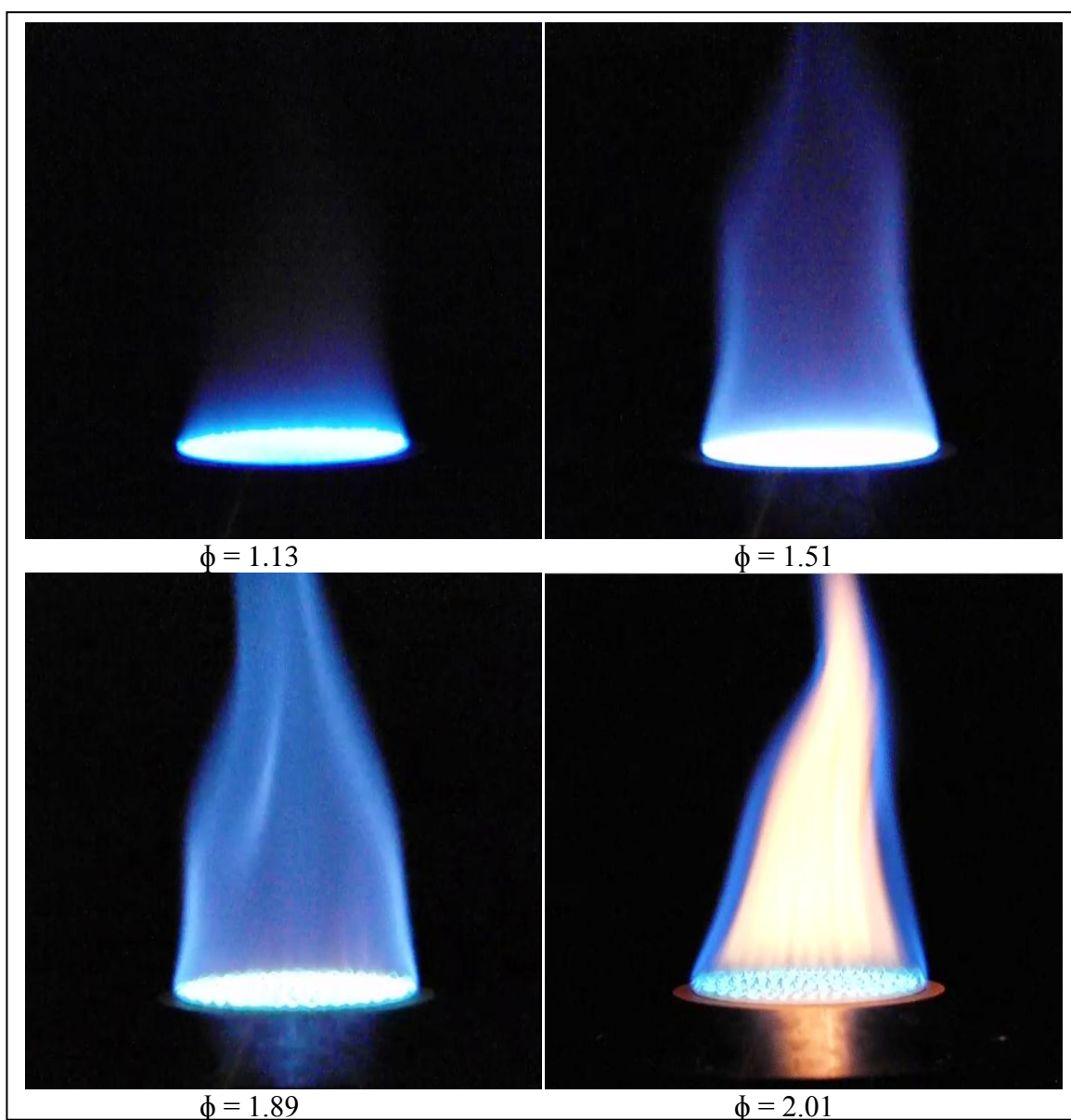


Figure 4.2: Flame images for premixed iso-octane fuel at the given equivalence ratios

Apart from n-heptane and iso-octane, some other PRF mixtures and toluene fuel were also tested. A typical image obtained from PRF 80, i.e. 80% iso-octane and 20% n-heptane by volume is displayed and analyzed as follows.

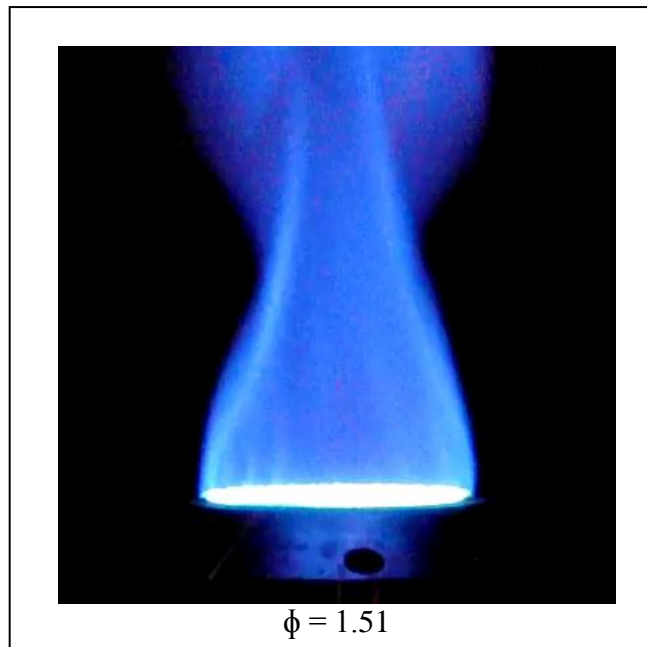


Figure 4.3: Flame image for premixed PRF 80 at the ER =1.51

The flame at all stages of PRF 80 appeared to be similar to PRF 100 as expected. Other combinations of fuel and air to give same equivalence ratios were also tested. For example, a fuel flow rate of 6.25 ml/min of iso-octane and 37 ml/min airflow is also at stoichiometric ratio and produced similar flame. The difference was in the fuel air mixture exit velocity. With fuel and air flows, the exit velocity increased and a little more turbulence was seen near the tip of the flame. Airflow rate being the dominant of the two was the primary driving factor of increasing mixture exit velocity. Due to this reason, only certain conditions of fuel air flow rates and mixture velocities were tested as they produced the ideal and most stable flames.

Toluene fuel was tested last because of its unpredicted behavior due to octane number being higher than 100. The flame for toluene appeared very different than iso-octane and n-heptane at the equivalence ratio of 1.51. Yellow streaks of flames appeared in the core of the blue flame whereas; the flames for both n-heptane and iso-octane were stable and appeared dark blue. Upon increasing the equivalence ratio to 2.01, the flame turned bright yellow red producing smoke and left soot deposits on the burner which made us discontinue the testing of toluene fuel.

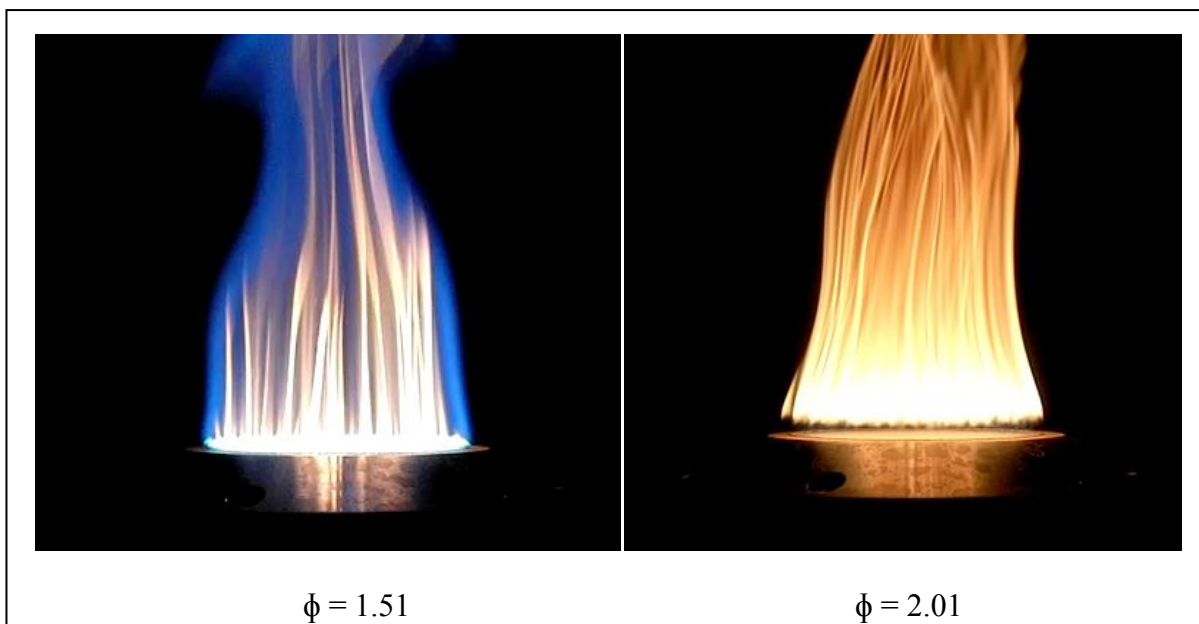


Figure 4.4: Flame images for premixed toluene fuel at the given equivalence ratios

4.2 Flame Liftoff

Flame lifting depends on a local flame and flow properties near the edges of the burner port. On a circular tube at low flow velocities the edge of the flame lies quite close to the burner lip and is said to be attached. When the velocity is increased, the cone angle of the flame decreases and the edge of the flame is displaced a small distance downstream. With further increases in the flow velocity, a critical velocity is reached where the flame edge jumps to this position, it is said to be lifted. Increasing the velocity beyond the lift-off value results in increasing the lift-off distance until the flame abruptly blows off the burner altogether.

After the initial step of flame analysis and visualization, the secondary gas from the shroud ring around the burner plug was introduced. The shroud gas at room temperature provided as a medium of thermal quenching of the premixed flame. Using a small computational study, it was determined that the shroud gas flow intended to move towards the center of the burner plug and in the process caused flame lift-off. The interaction between the hot gaseous products in the premixed flame and the relatively colder shroud gas became the cause of thermal quenching. From the literature section describing the study performed by Halstead et al. (1971), it can be deduced that quenching affects the thermal run away condition. The shield gas will change the thermal run away condition. By controlling the velocity of the secondary or shroud gas from the burner, the amount of quenching could be increased or decreased which was seen as the flame lift-off distance. Thus, when the shroud gas velocity was increased keeping the fuel-air mixture velocity constant, the lift off distance became larger and when the when the velocity of the shroud gas was turned off, the flame would fall back on to the burner base. This phenomenon provided us with the indication to study the behavior of PRF mixtures with different octane numbers towards their quenching capabilities.

At first, PRF 0 (n-heptane) was tested at different equivalence ratios and with different mixture exit velocities. After performing several tests, it was determined that equivalence ratio of 1.51 gave the most prominent results in terms of lift-off which could be compared to other PRF ratios. The secondary gas used for the first set of tests was nitrogen taken at room temperature and transported through a series of tygon and steel tubing up to the burner shroud ring. The input fuel feed rate for n-heptane was fixed at 6.25 ml/min and air flowrate at 36 l/min and the nitrogen velocity was increased from 0 to about three times the fuel-air mixture velocity at the burner exit.

Figure 4.5 shows lift-off images for n-heptane with nitrogen co-flow. With no nitrogen velocity, the flame rests steadily on the burner base. As the velocity is increased to 0.12 m/s, the edges of the flame are seen lifted with the bright disc still attached to the base. At 0.24 m/s nitrogen co-flow, a clear gap could be observed between the bright white disc that rests on the burner base and the lifted blue n-heptane flame. The fuel air mixture velocity with the given flow rates is 0.22 m/s. When the nitrogen velocity is increased beyond this velocity, the lift off distance is seen to increase up to almost two inches above the burner base. This also accounts for the turbulence seen as the velocities at this point are much higher for the flame to remain stable.

In order to test the maximum lift off capability of the flame at these conditions, the nitrogen velocity is furthered increased up till its triple the fuel air mixture velocity. At this velocity, an enormous amount of turbulence is seen and the flame lift-off distance is seen to be the maximum. Any further increases to the velocity would take the flame to blowoff condition making it highly unstable. It should be noted that in all these test conditions, the bright white disc was never lifted. The cup like structures near the base of the flame stretched when the flame separation distance increased due to interaction with the inert gas particles and increasing instabilities with higher velocities.

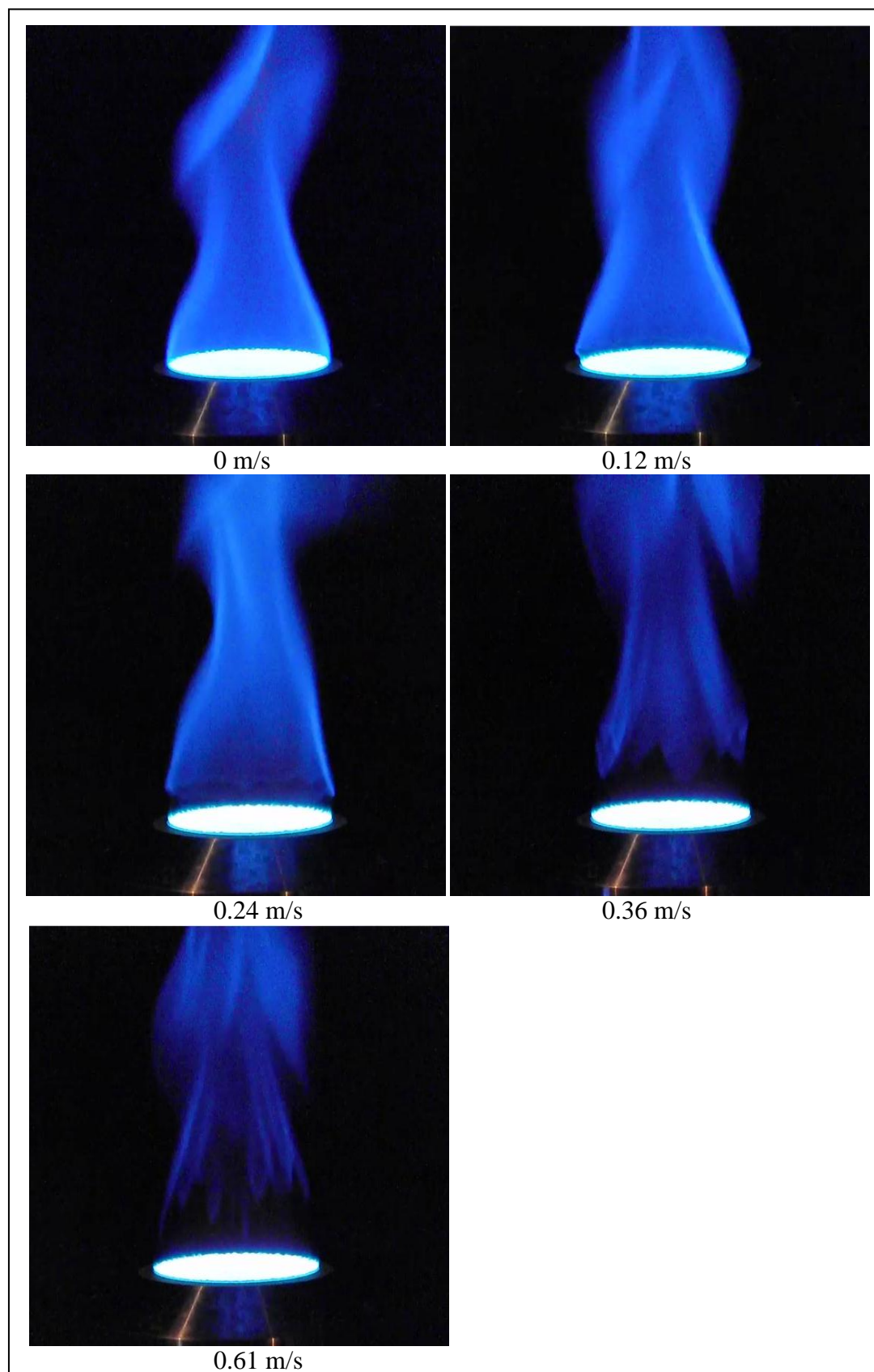


Figure 4.5: Flame lift off images for PRF 0 with nitrogen co-flow

Next set of images (Figure 4.6) are for iso-octane with a co-flow of nitrogen. The input fuel flow rate was set to be same as n-heptane at 6.25 ml/min with air flow at 37 l/min at equivalence ratio of 1.51. Iso-octane flame had slightly different appearances as studied in the first section of this chapter; it also behaved differently during lift-off process.

At 0 m/s nitrogen velocity, the flame is seen to be stable and resting on the burner base similar to n-heptane flame. When the nitrogen velocity is increased to 0.12 m/s, very minute separation is seen near the edges of the flame. Again, the bright disc is not affected by the lift-off and is seen sitting on the burner base. After increasing the velocity to 0.24 m/s, the iso-octane flame lifts up as well but the central flame is seen attached to the bright disc. A light thin film of blue flame shaped as a hemisphere extends outward from the flat bright flame and is always attached to the lifted flame in the middle. Similar behavior is seen when the nitrogen velocity is increased even more to 0.36 m/s and 0.61 m/s. The flame does lift up but the inner blue flame tries to attach itself to the lifted flame unlike n-heptane where the flames, that is, the bright flat flame and the lifted blue flame were entirely separated during lift-off. Very high amount of turbulence is also seen in the flame when the nitrogen velocity is increased to triple the fuel air mixture velocity at 0.61 m/s. The flame here is finally able to detach itself to the light blue flame. These images provided as a starting point where some differentiation could be made between different ratios of PRF fuels and their lift off capabilities. In order to observe the quenching from a different perspective, a spectrometer was used to study spontaneous emissions at different wavelengths. The spectrometer served as a validation to our camera collected images as it demonstrated similar differences between the two tested fuels.

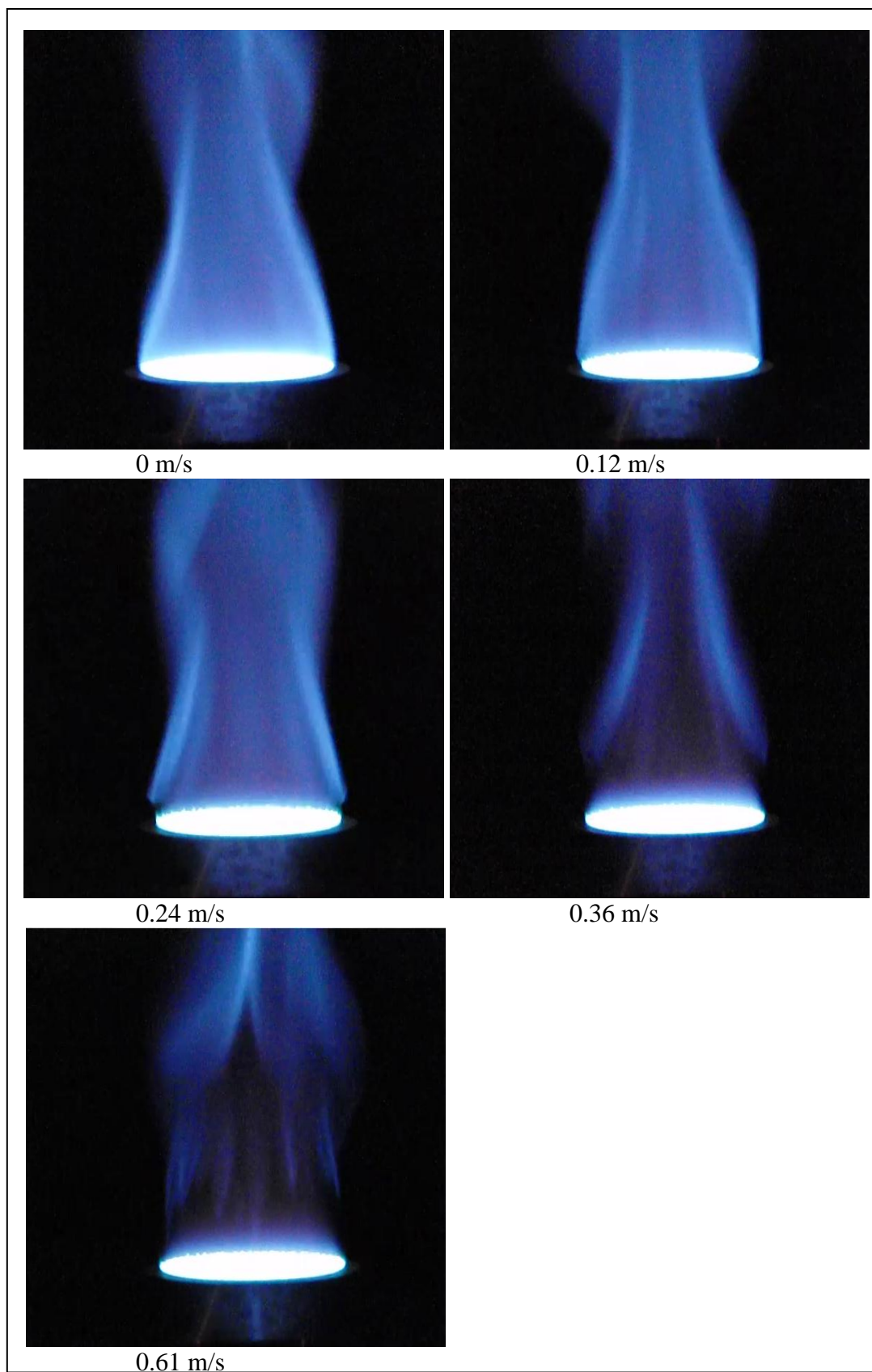


Figure 4.6: Flame lift off images for PRF 100 with nitrogen co-flow

4.3 Spectrometer

The spectrometer was set on top of a stand parallel to the flame length and the camera was placed adjacent to the viewing lens of the spectrometer for taking pictures. Once the flame was produced, the dial on the spectrometer was used to alter the wavelength. Certain radical species such as CH^* and OH^* give off radiation at specific wavelengths which are detected by the spectrometer. The lower and upper limits for the wavelengths were simply set by the onset of an image on the screen. The dial was increased in increments of 25 nm. The tests were performed at equivalence ratio 1.51, 1.89 and 2.01. As quenching a flame close to stoichiometric was very difficult, therefore mixtures with equivalence ratio lower than 1.51 was neglected. Tests were also categorized by images taken with and without nitrogen co-flow. Following are the set of images for n-heptane without nitrogen co-flow at equivalence ratio of 1.51.

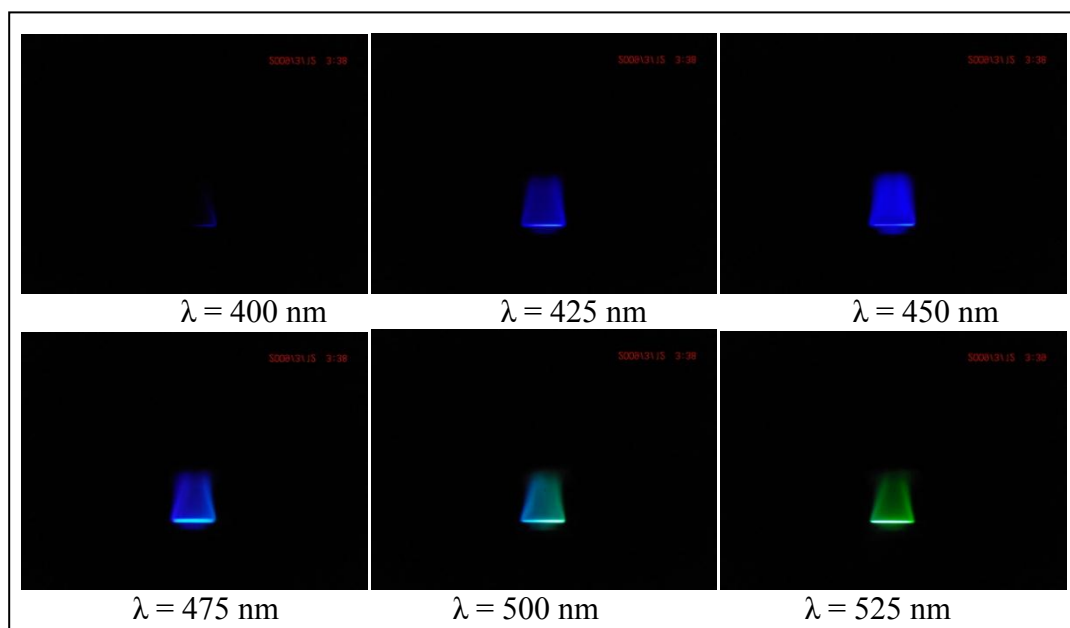
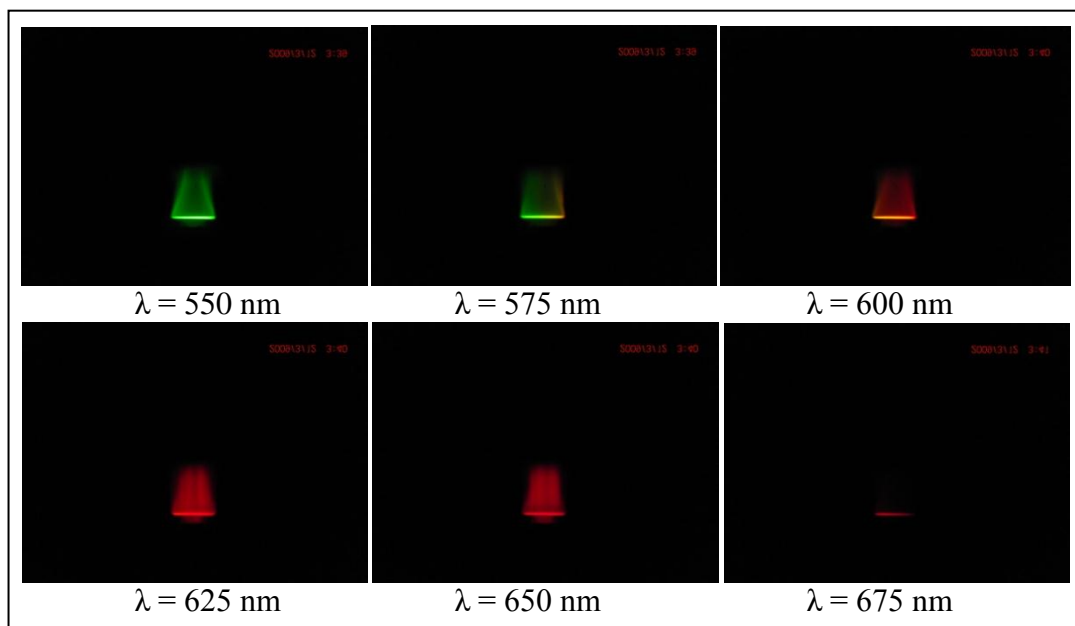


Figure 4.7: Flame images from spectrometer for n-heptane with no nitrogen co-flow

Figure 4.7 - Continued



From the set of images above for n-heptane with no nitrogen flow, several observations could be made. The emissions start becoming visible from a wavelength of 400 nm and appear until 675 nm defining the range for PRF 0 fuels at equivalence ratio 1.51. The colors of the flame change from blue towards red following the VIBGYOR spectrum. The intensity and the length of the flame image captured also determine the composition of the flame. The images with full flame length and bold colors determine that radical emissions at those particular wavelengths are more prominent in the flame. Next set of images are presented for iso-octane with no nitrogen co-flow at equivalence ratio of 1.51 for comparison.

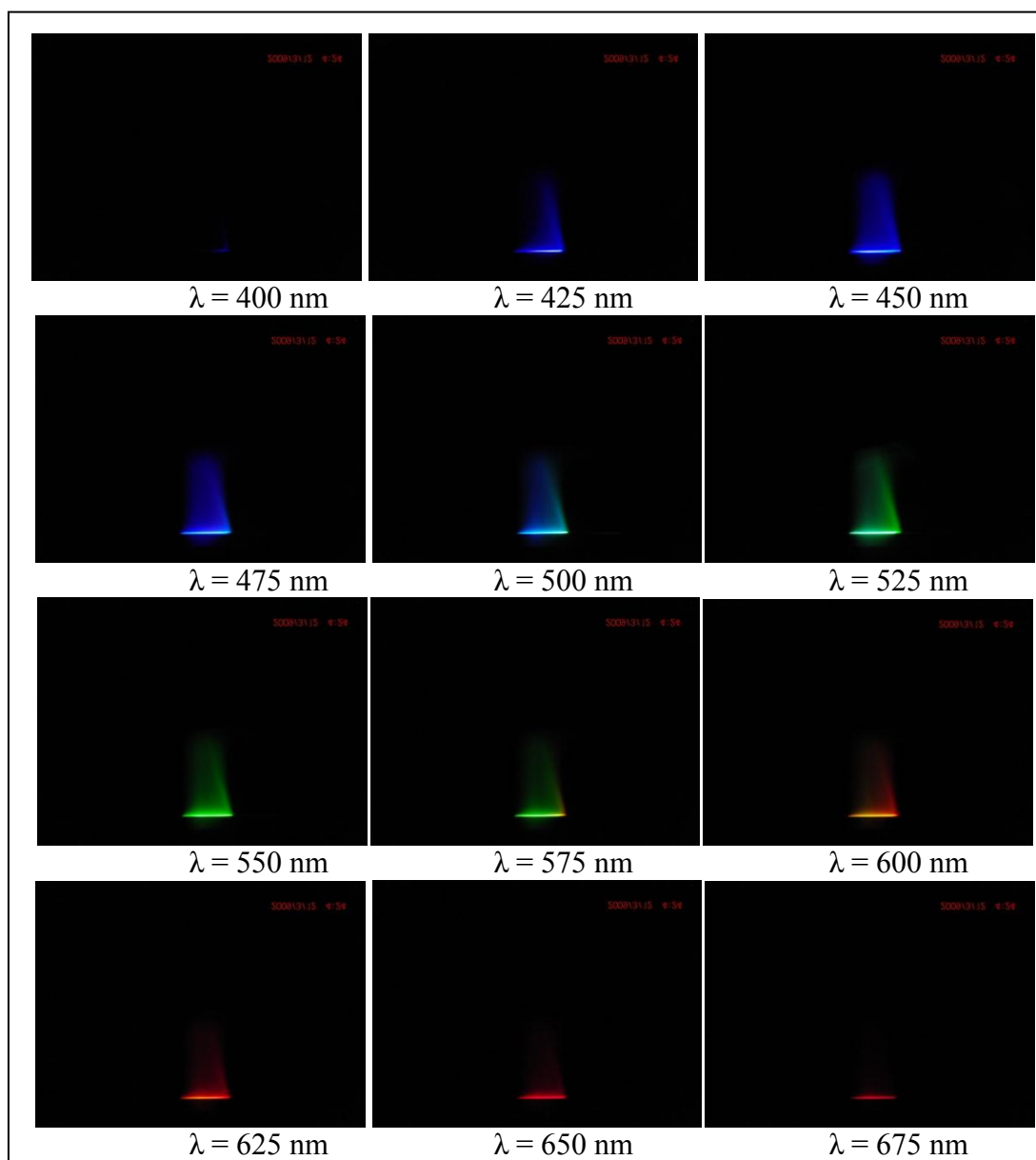


Figure 4.8: Flame images from spectrometer for iso-octane with no nitrogen co-flow

In the case presented above, the transition to light blue or green starts at 525 nm for n-heptane where as it is in between 525 and 550 nm for iso-octane. Similarly, from green to red transition falls at 600 nm for n-heptane, while occurring between 600 and 625 nm for iso-octane. It was also noted that, the emissions corresponding to higher wavelengths (red) were less for iso-octane than n-heptane.

Next the nitrogen co-flow was turned on at a velocity equal to the fuel air mixture velocity at the exit of about 0.22 m/s. Following images are for n-heptane at equivalence ratio of 1.51 with nitrogen co-flow.

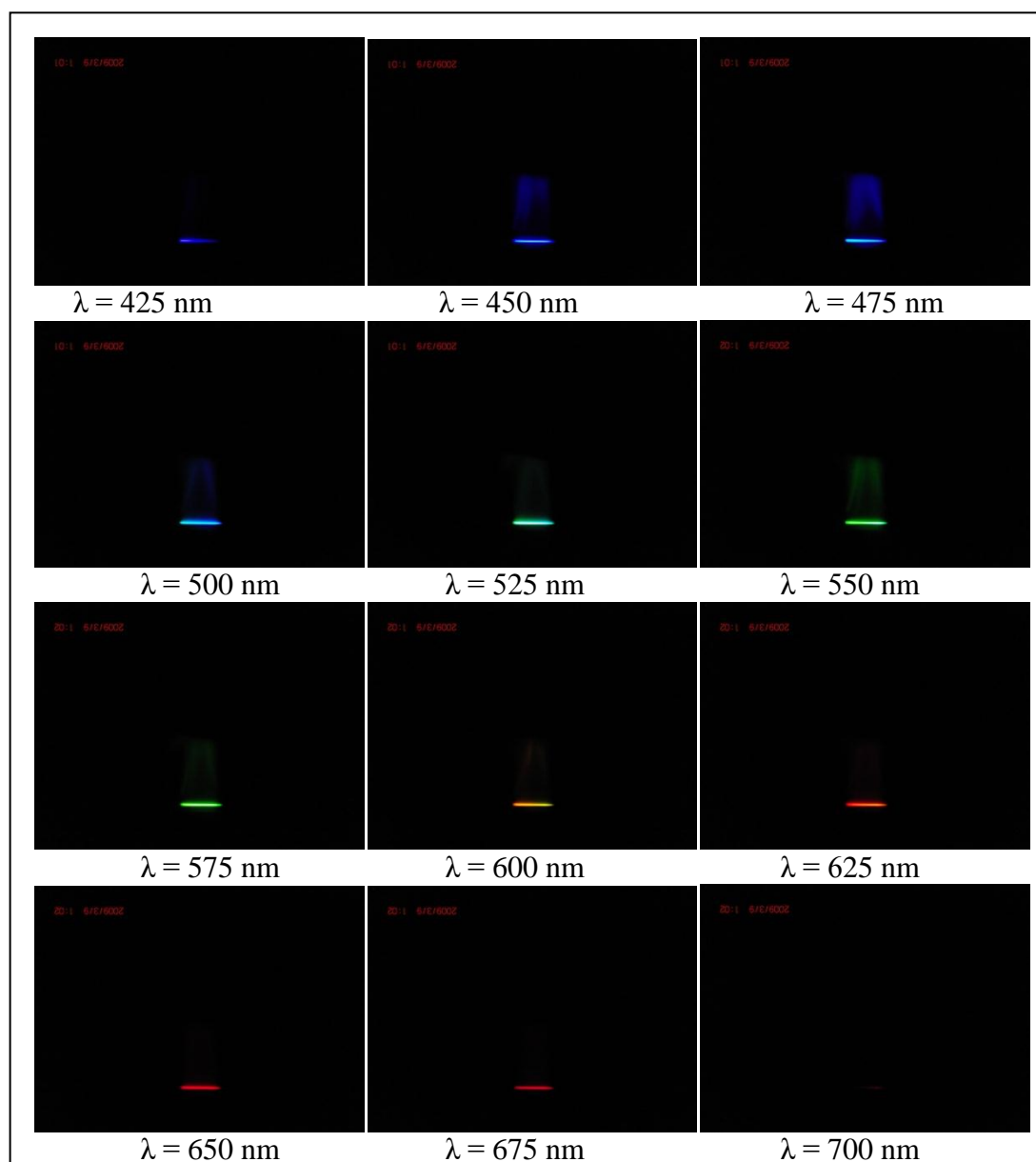


Figure 4.9: Flame images from spectrometer for n-heptane with nitrogen co-flow

With the co-flow of nitrogen, the wavelength scale where earlier pictures were retrieved shifted by an increment of 25 nm. The emissions with nitrogen flow appeared for wavelengths ranging from 425 nm to 700 nm. Emissions only at wavelengths 450-475 nm and 550-600 nm showed the flame being quenched. Other images at all the other wavelengths still seemed to be attached to the flat flame. Iso-octane was tested with similar conditions in order to find out if the difference in quenching capabilities still existed when put under the lens of a spectrometer. These are displayed in Figure 4.10.

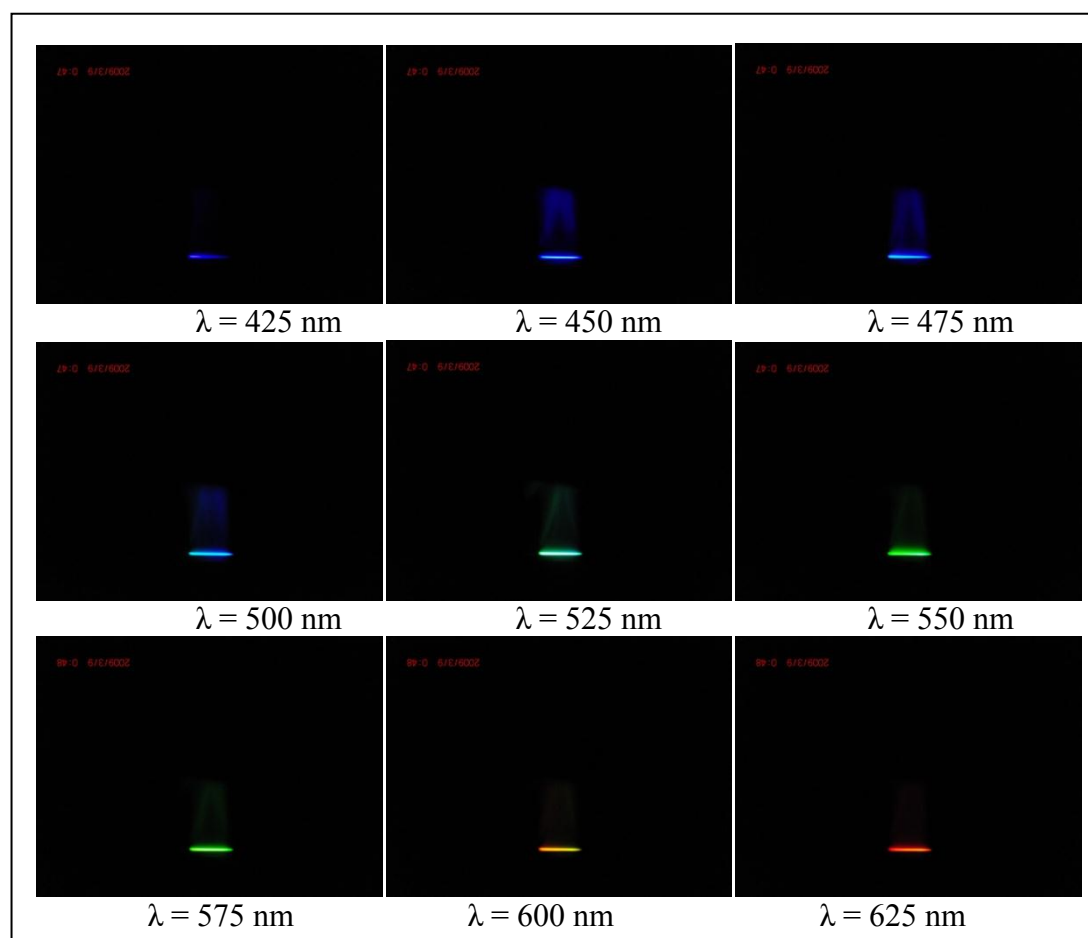
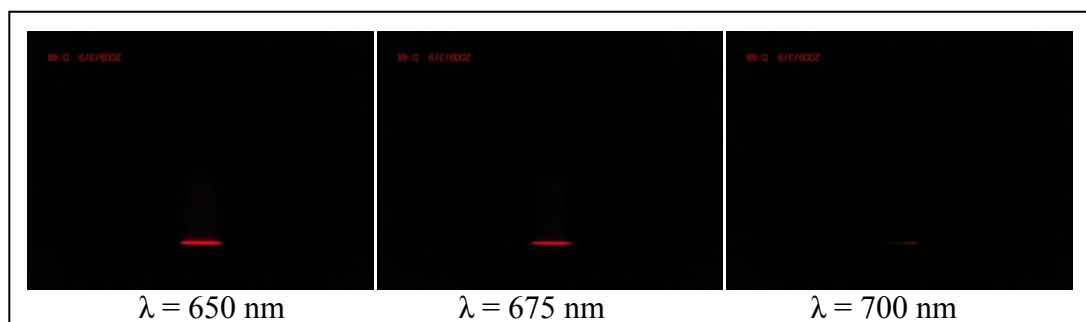


Figure 4.10: Flame images from spectrometer for iso-octane with nitrogen co-flow

Figure 4.10 - Continued



The shift in the wavelength scale was noted for iso-octane as well. Images captured at wavelengths of 475 nm and 550 nm for iso-octane when compared to n-heptane showed a clear cut difference in the amounts of quenching capabilities of the two fuels using the same method. N-heptane was much easier to quench than iso-octane which was prominent at these two wavelengths. The blown up images at these two respective wavelengths are shown again as follows that quantify the hypothesis of difference in quenching for different octane number fuels.

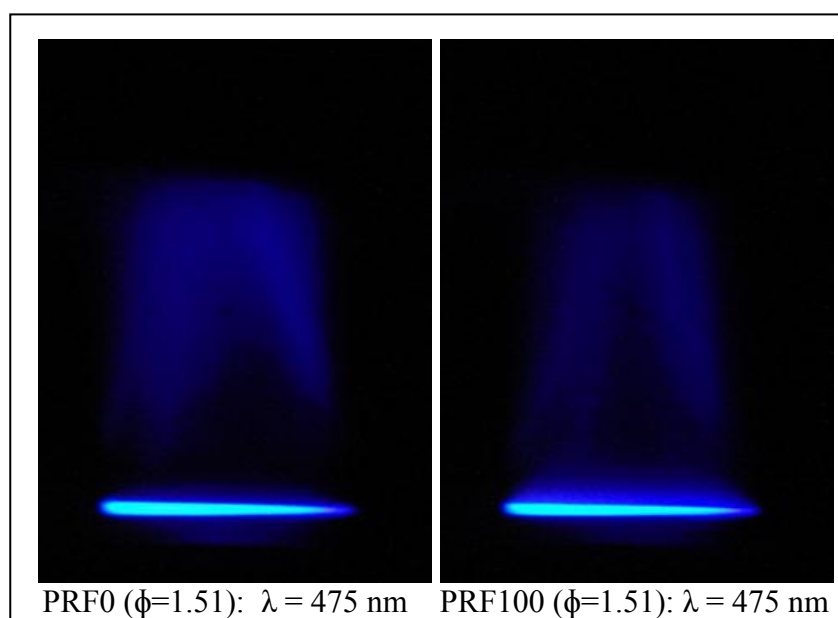
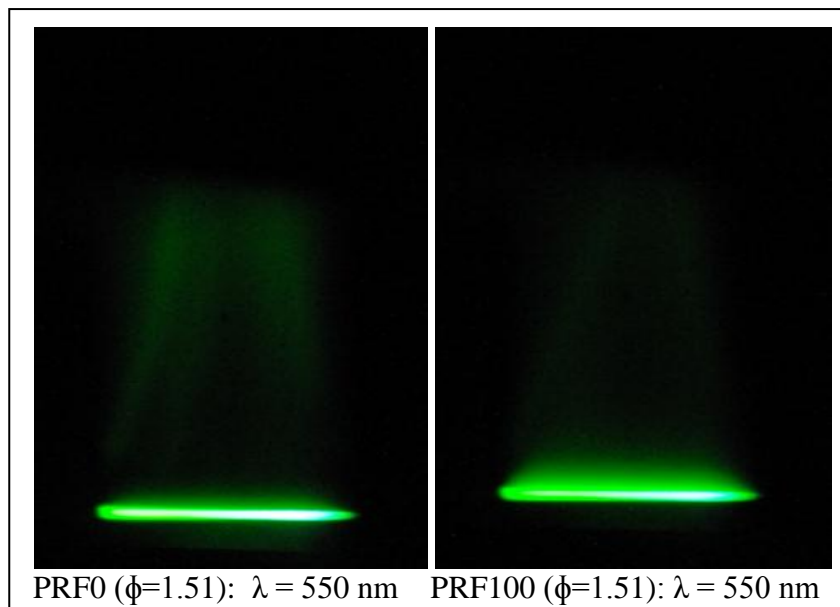


Figure 4.11: Flame images from spectrometer for PRF 0 and PRF 100 at ER = 1.51 showing difference in lift of at wavelengths of 475 nm and 550 nm

Figure 4.11 - Continued



The spectrometer tests were also performed for rich mixtures of PRF fuels. With higher equivalence ratio, similar quenching results were seen but at a lower wavelength. The following images are for n-heptane and iso-octane with an equivalence ratio of 2.01 and at wavelength of 425 nm.

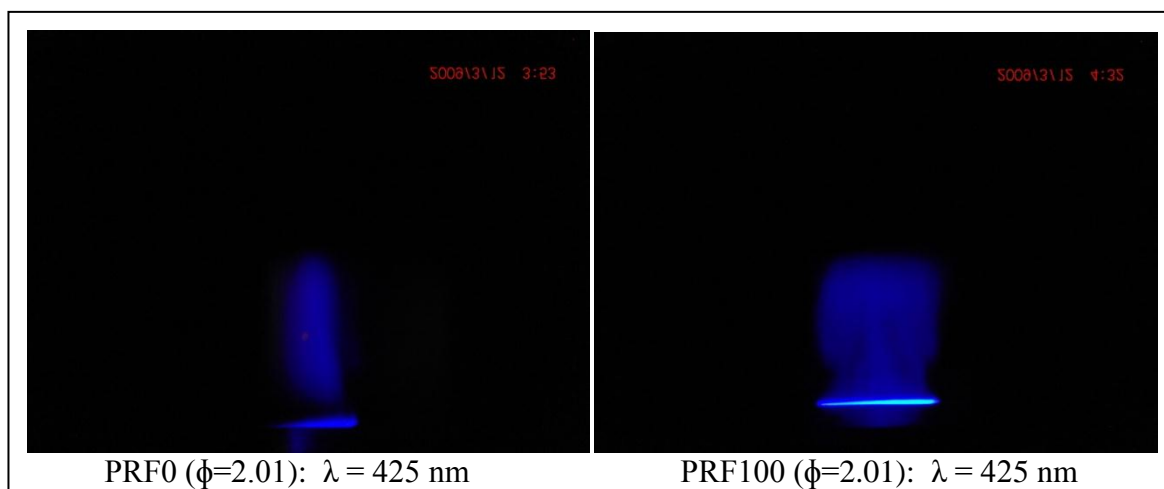


Figure 4.12: Flame images from spectrometer for PRF 0 and PRF 100 at ER = 2.01 at wavelength of 425 nm

At last, toluene flame was looked through the spectrometer as well to see if there is any quenching at all for a fuel with octane number higher than 100. With iso-octane with octane rating of 100 showing very minimal lift off, it was expected to see no or even less lift off with toluene. Following set of images display the spectrometer pictures for toluene at equivalence ratio 1.51 with a co-flow of nitrogen.

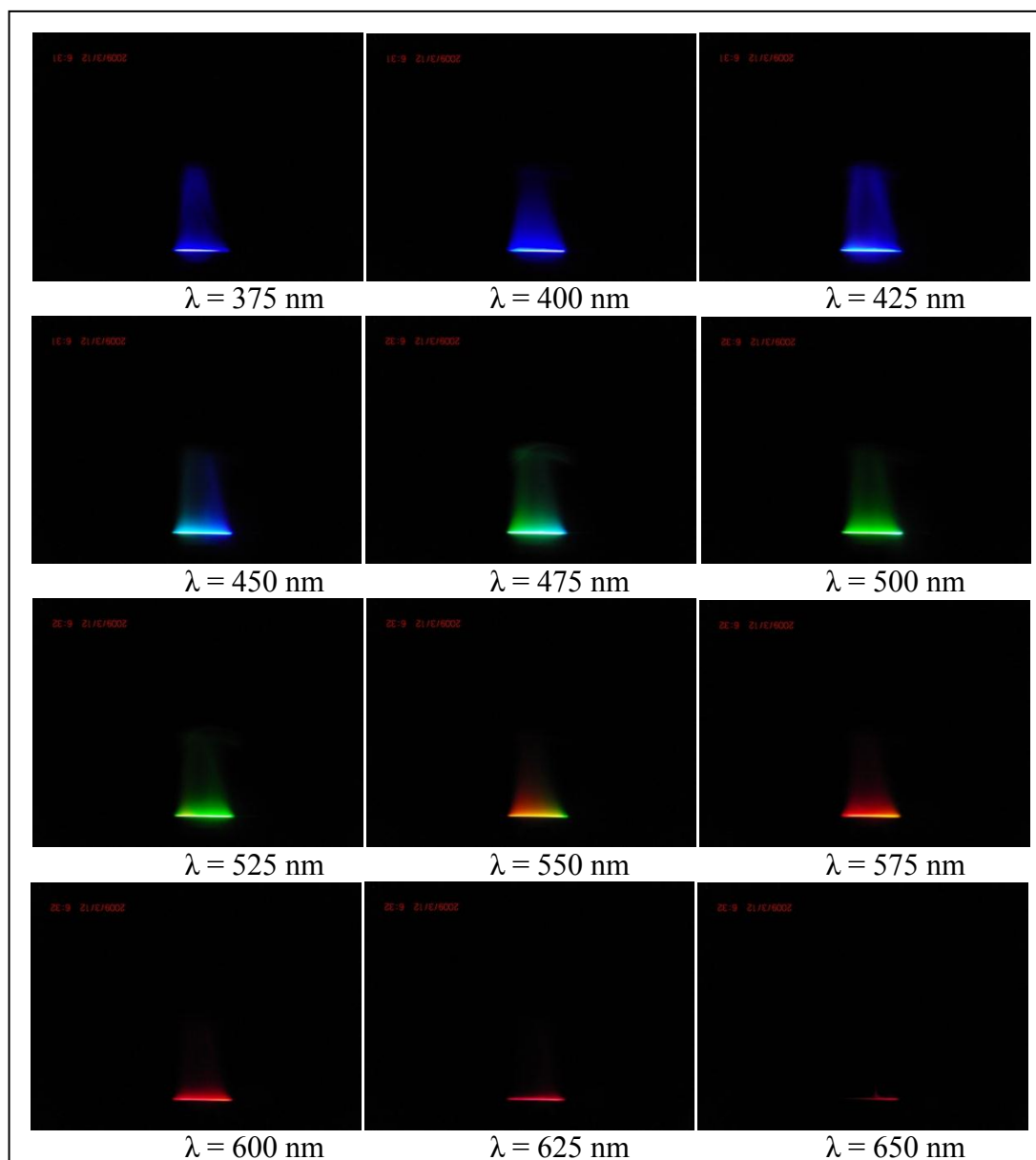


Figure 4.13: Flame images from spectrometer for toluene with nitrogen co-flow

The upper and lower limits on the wavelength where an image could be taken was 375 nm and 650 nm for toluene compared to 425 nm and 700 nm with n-heptane and iso-octane with co-flow. As expected, no lift off was seen for a higher octane rating fuel. As for any experimental study, repeatability is essential and hence these tests were conducted several times and identical results were obtained. The results from the spectrometer validated the hypothesis that lower octane number fuels are easier to quench than higher octane number fuels. Next section presents these results in a quantified form showing various trends between octane rating of fuels, equivalence ratios, quenching, and secondary gas velocities.

4.4 Octane Rating vs. Quenching

In this section, the trends for various primary reference fuels with different octane ratings and their quenching capabilities over a wide range of equivalence ratios are shown. The flame lift-off using camera and spectrometer sections focused on quenching results at equivalence ratio of 1.51 as that particular ratio gave the best possible visual confirmations of the quenching phenomenon. But in order to get a curve for lift-off versus different octane rating fuels, a range of equivalence ratios were tested. This was done by keeping the fuel flow fixed and increasing the air flow to get a range of equivalence ratios. At each condition, the secondary gas velocity, nitrogen or helium, were increased in order to test two different stages in the flame lift-off. The first stage was recorded when the flame just starts to lift off the edges which for any given fuel at a given equivalence ratio states the minimum amount of secondary velocity needed to lift off the flame from the burner base. The second stage was recorded when the secondary gas velocity was enough to lift the flame completely of the burner base that is seen in sections above with equal secondary gas and fuel air mixture exit velocity. At first, PRF 0 and PRF 100 were tested and compared with a co-flow of nitrogen.

Table 4.3: Data for lift-off with PRF 0 and PRF 100 with N₂ co-flow

Fuel = 6.25 ml/min	PRF 0	PRF 100	Starting to Lift- N2 velocity [m/s]		Lifted- N2 velocity [m/s]		Mixture velocity [m/s]	
			PRF 0	PRF 100	PRF 0	PRF 100	PRF 0	PRF 100
Air [l/min]	ER	ER						
20	2.73	2.79	0.037	0.037	0.092	0.098	0.125	0.124
25	2.19	2.23	0.037	0.037	0.092	0.147	0.154	0.153
26	2.10	2.14	0.037	0.049	0.147	0.196	0.160	0.159
27	2.02	2.06	0.037	0.049	0.159	0.196	0.166	0.165
28	1.95	1.99	0.049	0.049	0.196	0.220	0.172	0.171
29	1.88	1.92	0.049	0.055	0.196	0.220	0.178	0.177
30	1.82	1.86	0.049	0.055	0.208	0.233	0.183	0.182
31	1.76	1.80	0.049	0.055	0.208	0.251	0.189	0.188
32	1.71	1.74	0.055	0.080	0.208	0.251	0.195	0.194
33	1.66	1.69	0.055	0.080	0.208	0.300	0.201	0.200
34	1.61	1.64	0.061	0.092	0.233	0.306	0.207	0.206
35	1.56	1.59	0.061	0.110	0.233		0.212	0.211
36	1.52	1.55	0.073		0.257		0.218	0.217
37	1.48	1.51	0.098				0.224	0.223

It is seen from the table above that for each set of fuel and air ratio, the equivalence ratio differed for iso-octane and n-heptane due to difference in their properties. Nitrogen flow rate was recorded at each step for ‘starting to lift’ and ‘lifted’ conditions and was then converted into velocity with the known annulus area. The two conditions are compared and plotted in the chart below.

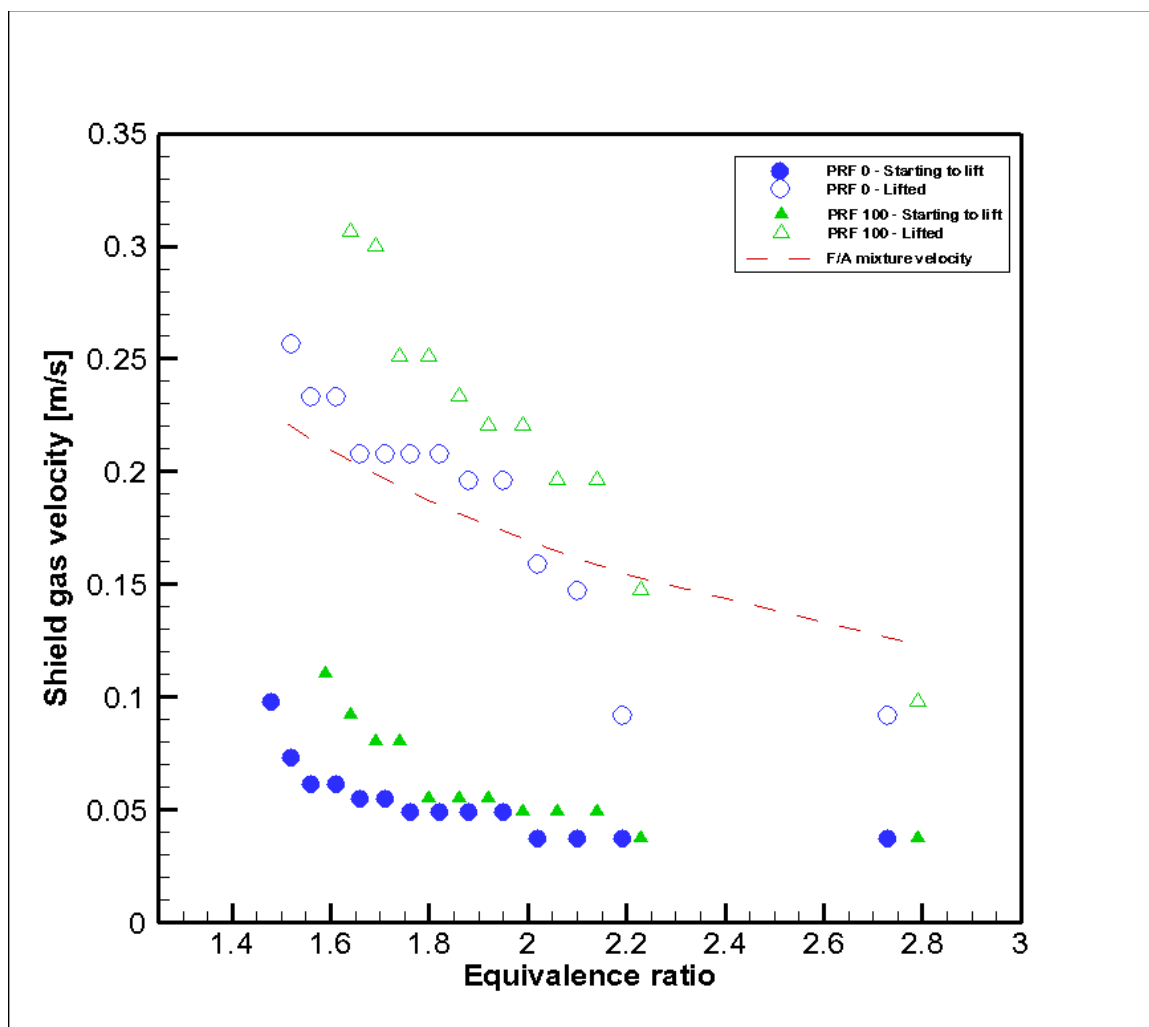


Figure 4.14: Lift-off with nitrogen vs. equivalence ratio for PRF 0, 100

The equivalence ratios ranged from 1.48 (PRF 0) and 1.51 (PRF 100) that was the closest to stoichiometric ratio where lift off was possible up to rich ratios of 2.73 (PRF 0) and 2.79 (PRF 100). At any given equivalence ratio, the velocity needed to completely lift the flame was much higher than to just the lift the edges. But the gap between the velocities at two stages narrows down as the equivalence ratio increases due to the decreasing fuel-air mixture velocity. It could be noted from the figure that higher quenching velocities are needed than the fuel-air mixture velocity when equivalence ratio is less than 2.02 for n-heptane and 2.23 for iso-octane. Beyond these equivalence ratios,

shield gas velocities needed to lift up the flame are lower than the fuel-air mixture exit velocity. The main difference in quenching between a fuel with an octane rating of 0 and 100 that was seen using a high definition camera and a spectrometer is confirmed and quantified by this plot. It is easier to quench lower octane number fuels such as n-heptane than higher octane number fuels like iso-octane. Higher velocities of nitrogen were needed to start the lift off of an iso-octane flame and also to completely lift the octane flame compared to heptane flame. This difference is again higher when the exit fuel-air mixture velocities are higher. The velocities needed to lift up the flame become constant after an equivalence ratio of about 2.2 for both iso-octane and n-heptane up till an equivalence ratio of 2.79 is reached. Beyond this ratio, the flame is too rich for any quenching to be observed.

Once the relationship of octane rating versus quenching was established using the fuels at two extremes on the octane scale, some PRF ratios between 0 and 100 were prepared and tested. The next set of data is represented for PRF 65 and 85.

Table 4.4: Data for lift-off with PRF 65 and PRF 85 with N₂ co-flow

Fuel = 6.25	PRF65	PRF85	Starting to Lift- N2 velocity [m/s]		Lifted- N2 velocity [m/s]		Mixture velocity [m/s]	
	ER	ER	PRF 65	PRF 85	PRF 65	PRF 85	PRF 65	PRF 85
20	2.77	2.78	0.037	0.037	0.092	0.098	0.124	0.124
25	2.21	2.22	0.037	0.037	0.122	0.141	0.154	0.154
26	2.13	2.14	0.037	0.049	0.159	0.171	0.159	0.159
27	2.05	2.06	0.037	0.049	0.165	0.171	0.165	0.165
28	1.98	1.99	0.049	0.049	0.196	0.214	0.171	0.171
29	1.91	1.92	0.049	0.049	0.202	0.214	0.177	0.177
30	1.85	1.85	0.049	0.049	0.208	0.214	0.183	0.183
31	1.79	1.79	0.055	0.055	0.214	0.233	0.188	0.188
32	1.73	1.74	0.080	0.080	0.214	0.233	0.194	0.194

Table 4.4 - Continued

33	1.68	1.68	0.080	0.080	0.239	0.263	0.200	0.200
34	1.63	1.63	0.086	0.092	0.245	0.269	0.206	0.206
35	1.58	1.59	0.092	0.098	0.257	0.306	0.212	0.212
36	1.54	1.54	0.098	0.110	0.275		0.218	0.217
37	1.50	1.50	0.110				0.223	0.223

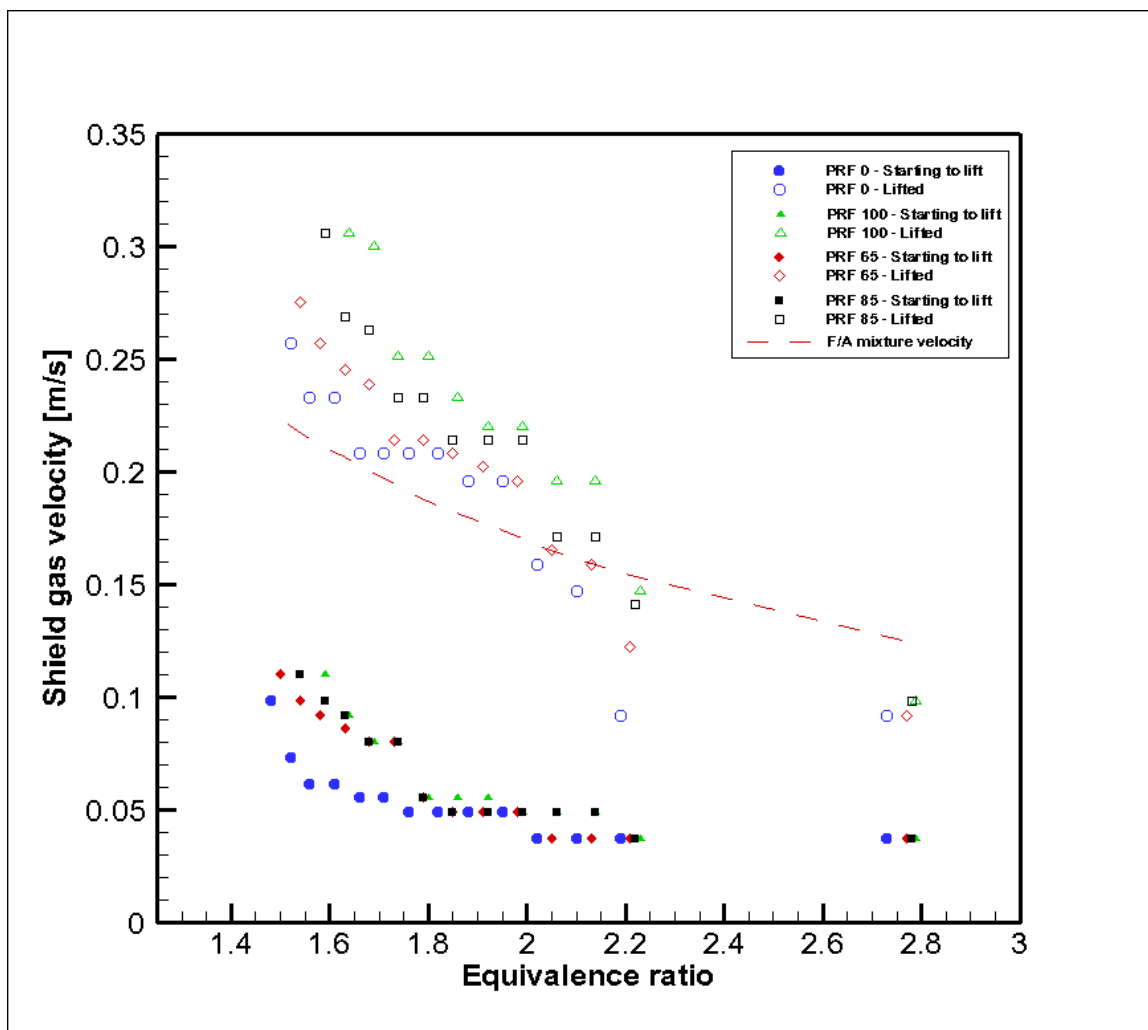


Figure 4.15: Lift-off with nitrogen vs. equivalence ratio for PRF 0, 65, 85 and 100

Figure 4.15 displays the quenching results of PRF 65 and 85 along with PRF 0 and PRF 100. The nitrogen velocities needed for lift-off of PRF 65 and 85 flames were always less than or equal to iso-octane and greater than or equal to n-heptane as expected. Higher nitrogen velocities were needed to lift the PRF 65 and PRF 85 flames than PRF 0 but lower than PRF 100. The difference between the lift off velocities for the middle two ratios decreases as the equivalence ratios are increased. At many equivalence ratios especially in the richer regime, required nitrogen velocities to slightly lift up the PRF 65 flame coincided with PRF 0 and PRF 85 coincided with iso-octane and sometimes both. For instance, at velocities lower than 0.15 m/s, the secondary gas velocity needed to lift up the flame was same for all PRF ratios and due to the flame richness and low fuel-air mixture velocity.

In order to increase the temperature difference for the thermal quenching to become more prominent, a lower specific heat gas was used. Helium having a lower specific heat capacity ($20.8 \text{ J mol}^{-1} \text{ K}^{-1}$ at $25 \text{ }^\circ\text{C}$) than nitrogen ($29.1 \text{ J mol}^{-1} \text{ K}^{-1}$ at $25 \text{ }^\circ\text{C}$) was expected to quench the fuels much easily with lower velocities. The following table displays the helium velocities needed to slightly lift and completely lift the PRF 0 and PRF 100 flames with varying equivalence ratios.

Table 4.5: Data for lift-off with PRF 0 and PRF 100 with He co-flow

F = 6.25	PRF 0	PRF 100	Starting to Lift- He velocity [m/s]		Lifted- He velocity [m/s]		Mixture velocity [m/s]	
	ER	ER	PRF0	PRF100	PRF0	PRF100	PRF 0	PRF 100
20	2.73	2.79	0.024	0.024	0.086	0.098	0.125	0.124
25	2.19	2.23	0.037	0.037	0.092	0.110	0.154	0.153
26	2.10	2.14	0.037	0.037	0.116	0.135	0.160	0.159
27	2.02	2.06	0.037	0.037	0.128	0.147	0.166	0.165
28	1.95	1.99	0.037	0.037	0.135	0.147	0.172	0.171

Table 4.5 - Continued

29	1.88	1.92	0.049	0.049	0.147	0.159	0.178	0.177
30	1.82	1.86	0.049	0.049	0.165	0.171	0.183	0.182
31	1.76	1.80	0.049	0.049	0.177	0.184	0.189	0.188
32	1.71	1.74	0.061	0.073	0.184	0.190	0.195	0.194
33	1.66	1.69	0.061	0.086	0.196	0.208	0.201	0.200
34	1.61	1.64	0.073	0.086	0.220	0.239	0.207	0.206
35	1.56	1.59	0.086	0.098	0.220	0.239	0.212	0.211
36	1.52	1.55	0.092	0.098	0.233	0.251	0.218	0.217
37	1.48	1.51	0.092	0.098	0.257	0.269	0.224	0.223
38	1.44	1.47	0.104	0.128	0.281	0.300	0.230	0.229
39	1.40	1.43	0.116	0.147	0.300	0.337	0.236	0.235
40	1.37	1.39	0.122	0.153	0.312		0.241	0.240
41	1.33	1.36	0.147				0.247	0.246

It could be seen from the data recorded that using helium as secondary gas, quenching was possible at equivalence ratios slightly less than 1.5 that was the lower limit with nitrogen. It was possible to lift up the edges of the n-heptane flame for an equivalence ratio of 1.33 with mixture velocities at 0.247 m/s. But the lowest equivalence ratio where the flame could be completely lifted was at 1.37 with helium gas velocity at 0.312 m/s for n-heptane compared to an even higher equivalence ratio of 1.43 for iso-octane which required a helium gas velocity of 0.337 m/s. At every point, the required helium gas velocity to quench the flame was much higher for iso-octane than n-heptane giving a clear relationship between the octane rating of the fuel and its quenching capabilities. Figure 4.16 shows the lift up plot with helium and PRF 0 and 100 fuels.

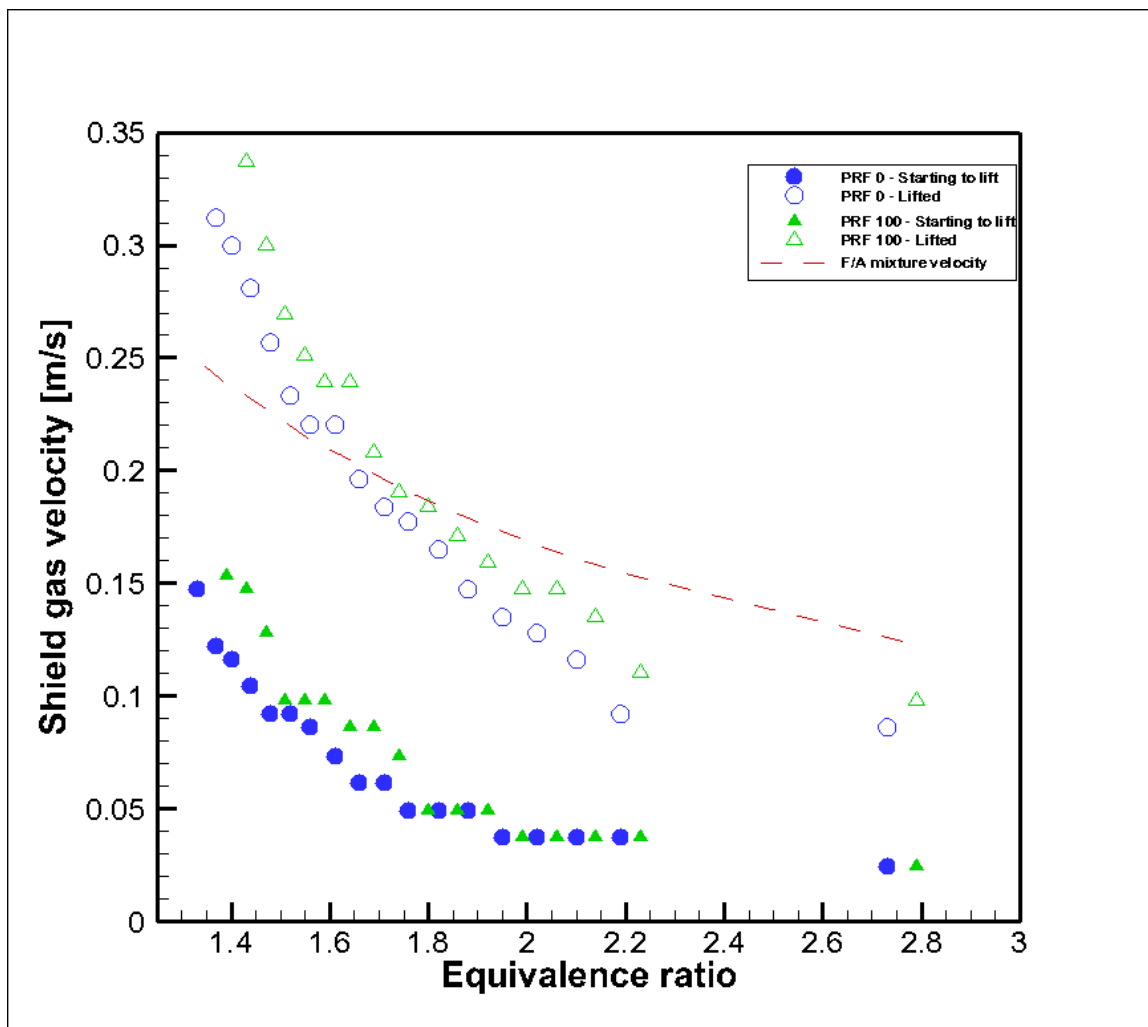


Figure 4.16: Lift-off with helium vs. equivalence ratio for PRF 0, 100

A more continuous slope was seen for quenching velocities versus the equivalence ratios when helium was employed. Although the difference of velocities needed to quench higher octane number fuels and lower octane number fuels was still present but at lower magnitudes. Therefore, the PRF 0 and PRF 100 quenching limits appeared to be very close to each other. The point after which the quenching velocities needed for lift up are lower than the exit fuel-air mixture velocities shifts back to about 1.7 equivalence ratio compared to about 2.2 in case of nitrogen.

Figure 4.17 shows the comparison of PRF fuels lift off capabilities with equivalence ratio between nitrogen and helium as the secondary gas flow. With helium, the flames could be lifted up at equivalence ratios ranging from 1.3 to 2.8 whereas the range was narrower for nitrogen of 1.5 to 2.8. This was due to helium being a lower specific heat gas was able to produce a higher temperature difference and hence was able to lift fuel-air mixtures relatively closer to stoichiometric ratios than compared to nitrogen. The difference between the initial lift up and completely lifted flame values remained fairly constant in case of helium. But when nitrogen was used, the difference was much larger at lower equivalence ratios and decreased with increasing equivalence ratio and finally became constant at equivalence ratio of 2.2. The difference between different octane number fuels, that is, iso-octane and n-heptane was larger at lower equivalence ratios and then gradually decreased with nitrogen, whereas it was constant throughout the range of equivalence ratios in the case of helium. Hence, due to the amounts of helium velocities needed to lift up the flames were so close to each other for PRF 0 and 100; it was assumed that PRF 65 and 85 would fall in the same scale of values as seen in the case of nitrogen.

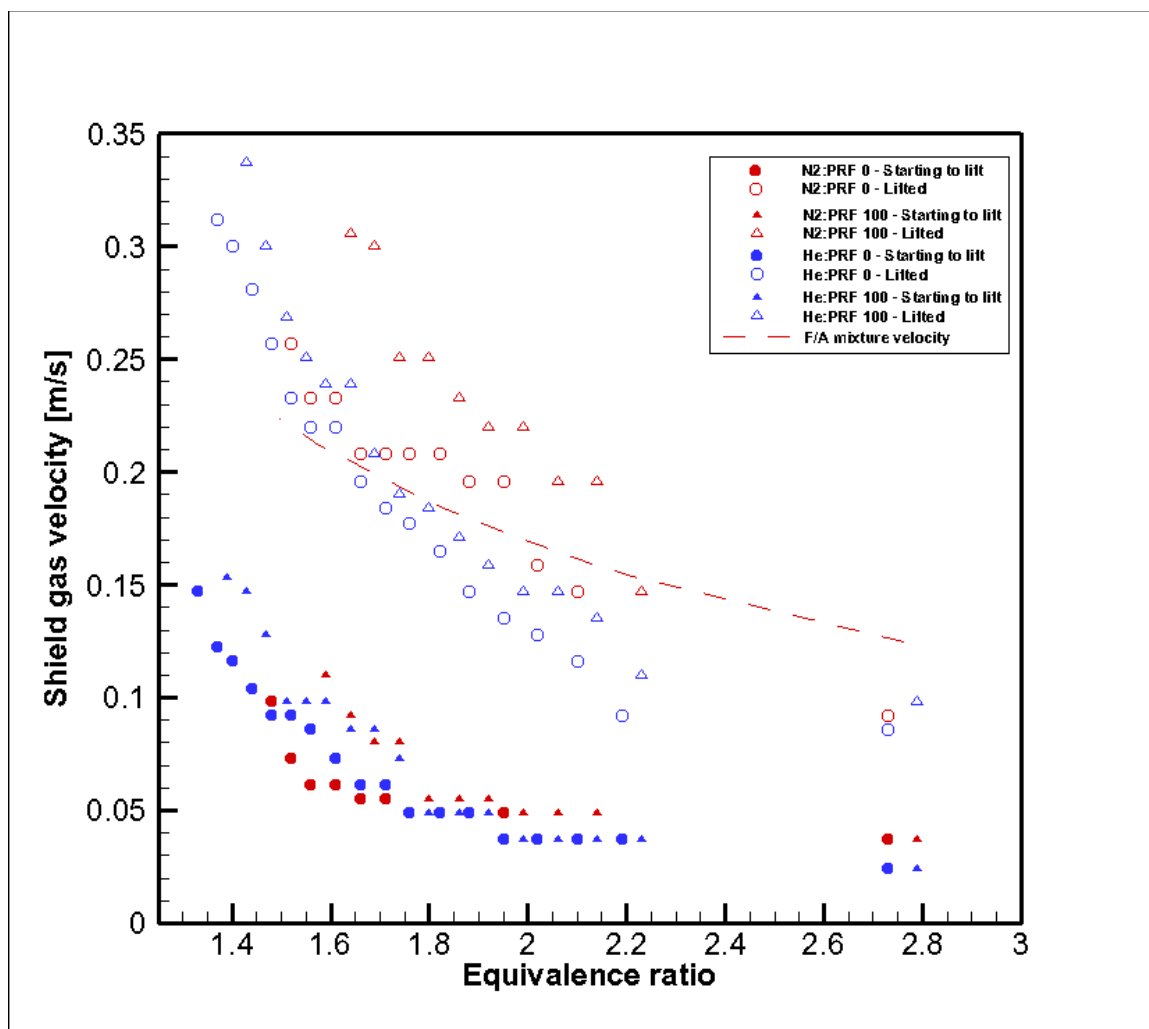


Figure 4.17: Difference in lift-off with N₂ and He as secondary gas velocity for PRF 0 and 100

At last, in order to confirm if the quenching method of octane number determination would also work for actual gasoline fuels that include many more hydrocarbons and additives other than iso-octane and n-heptane, gasoline 87 and 91 were purchased from a gas station and tested. Due to higher densities of gasoline compounds (711 kg/m^3 at 25 C), the equivalence ratio regime where quenching was possible was shorter for gasoline-air mixtures compared to PRF fuels. PRF fuels exhibited quenching for a range of $1.5 < \text{ER} < 2.8$ whereas gasoline fuels were limited to $1.8 < \text{ER} < 2.8$. The

following set of data and plot display the results for gasoline testing in comparison to PRF octane number prediction. It is seen that the octane number of the gasoline compounds can well be predicted if the test is run with the listed controlled conditions within a certain interval band of equivalence ratios. The values required for lifting up of the edges termed as ‘starting to lift’ above is neglected for next figure as the values were the same for gasoline and PRF fuels.

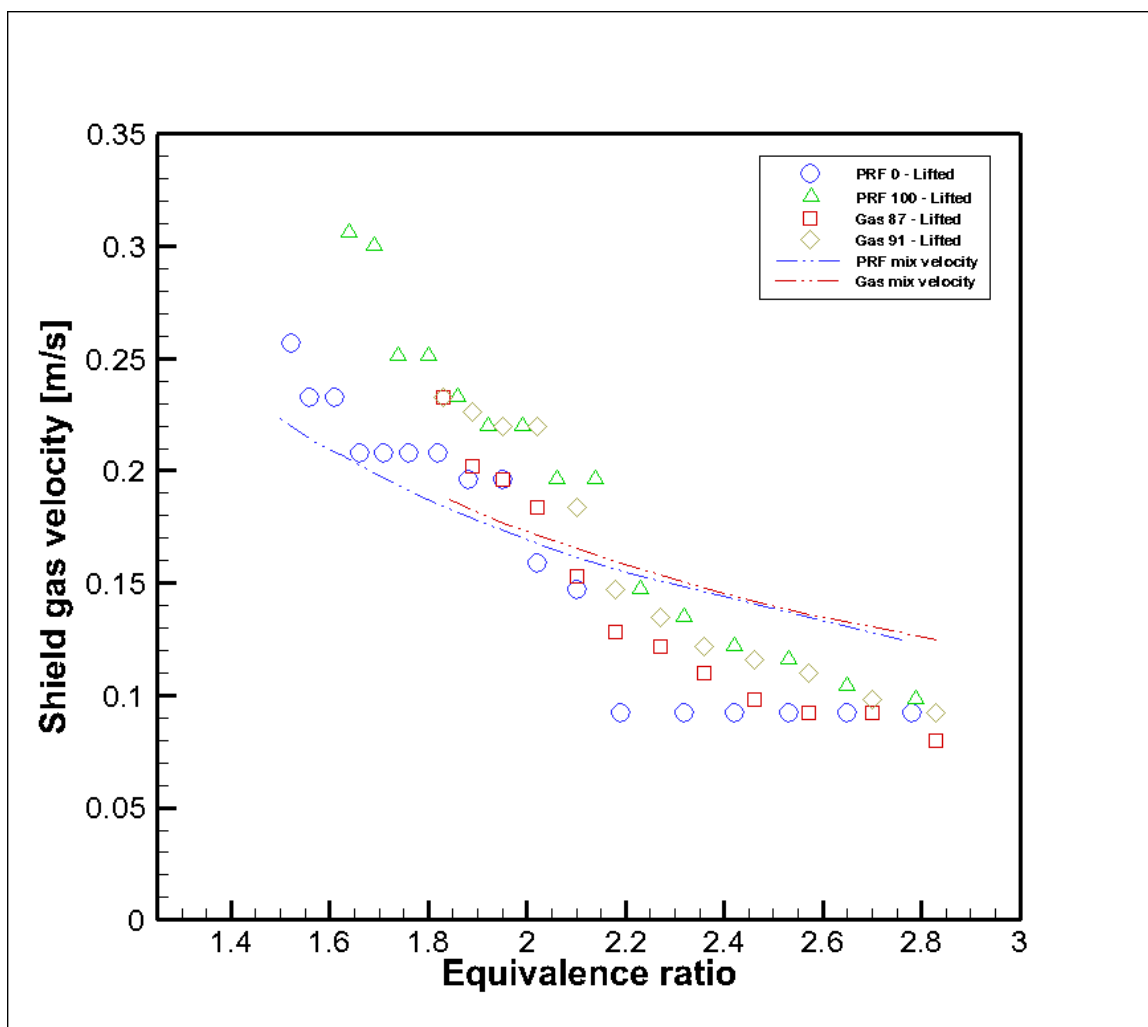


Figure 4.18: Lift-off with N_2 as shield gas velocity for Gasoline 87 and 91, PRF 0 and 100

Table 4.6: Data for lift-off with Gasoline 87 and 91 with N₂

Fuel = 6.25 ml/min	Gasoline 87			Gasoline 91			Mixture velocity [m/s]
	Air [l/min]	ER	Starting to lift – N ₂ velocity [m/s]	Lifted – N ₂ velocity [m/s]	ER	Starting to lift – N ₂ velocity [m/s]	
20	2.83	0.024	0.080	2.83	0.024	0.092	0.125
21	2.70	0.037	0.092	2.70	0.037	0.098	0.130
22	2.57	0.037	0.092	2.57	0.037	0.110	0.136
23	2.46	0.037	0.098	2.46	0.037	0.116	0.142
24	2.36	0.037	0.110	2.36	0.037	0.122	0.148
25	2.27	0.037	0.122	2.27	0.037	0.135	0.153
26	2.18	0.043	0.128	2.18	0.043	0.147	0.160
27	2.10	0.049	0.153	2.10	0.049	0.184	0.165
28	2.02	0.049	0.184	2.02	0.049	0.220	0.171
29	1.95	0.055	0.196	1.95	0.055	0.220	0.177
30	1.89	0.055	0.202	1.89	0.055	0.226	0.183
31	1.83	0.055	0.233	1.83	0.055	0.233	0.188

In order to clearly distinguish between the different octane number fuels with their quenching velocities needed for lift off, the above plot is shown with lines along with symbols in Figure 4.19. It can be seen that at certain equivalence ratios, it is quite easy to distinguish between the different gasoline compounds of different octane numbers based on their required quenching velocities.

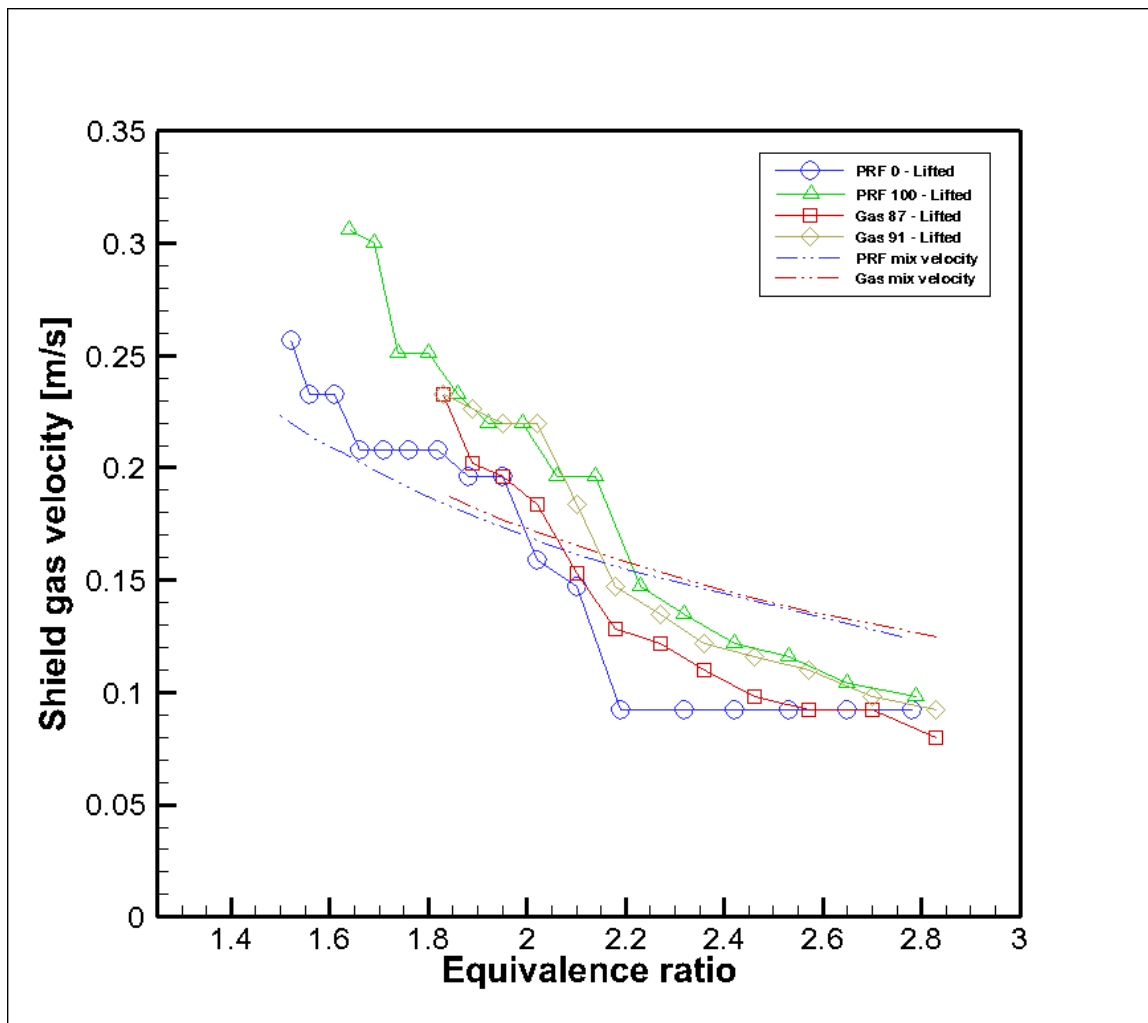


Figure 4.19: Lift-off with N_2 as shield gas velocity for Gasoline 87 and 91, PRF 0 and 100 with lines along with symbols

CHAPTER 5: CONCLUSIONS

Premixed combustion experiments were conducted on a flat flame burner with different primary reference fuels to determine the relation between octane rating of a fuel and its quenching by varying the velocity of a shielding gas stream around the premixed flame. The experimental results were analyzed using three different ways. The first compared the lift-off by using a high resolution camera and visualizing the lift-off of flames from the burner surface. The second method comprised of a spectrometer that measured the wavelengths of the radical species that contributed to quenching. The third method intended to quantify the above seen differences by quenching different octane ratio fuels on a wide range of equivalence ratios.

The FLUENT analysis of the flame quenching using premixed combustion model helped gain insight into mixing between the fuel-air mixture and the shielding nitrogen gas, and to aid determination of test conditions. The velocity vectors were seen to shield the flame only up till a distance of about 50 mm above the burner base. The velocities increased towards the center due to isotropic thermal expansion and upward buoyant acceleration. Lift off was explained by plotting x-velocities that showed inward movement of nitrogen gas in radial direction.

The high resolution camera used was able to capture the differences in lift off for iso-octane and n-heptane at equivalence ratio of 1.51. It was seen that the n-heptane flame would start to lift when nitrogen velocity was increased to 0.12 m/s, which was half the fuel-air mixture velocity and would be completely lifted when the nitrogen velocities were increased. Iso-octane flame on the other hand was much more difficult to lift with the same nitrogen co-flow, as a part of the central flame was attached to the base at all times that didn't let the flame lift off completely until nitrogen velocities were higher.

Through the spectrometer use, it was determined that radical species at wavelengths of 475 nm and 550 nm with an equivalence ratio of 1.51 were the key species taking part in the quenching phenomenon. It was proved that it was easier to quench the n-heptane flame compared to iso-octane flame. When the equivalence ratio was increased to a richer regime at 2.01, the image displaying wavelength of 425 nm showed prominent differences in lift-off between PRF 0 and 100.

Two secondary gasses including nitrogen and helium were used to quantify the quenching of different octane number fuel flames. With fuel flow rate fixed, air flow was controlled to test a wide range of equivalence ratios along with increasing secondary gas velocities to measure lift off. The velocities needed to lift up the flame completely at any given equivalence ratio was twice or more the amount needed to just lift the edges. The required velocity needed to lift up the flame increased with increasing octane number of the reference fuel taken. PRF 100 flame required the maximum secondary gas velocities followed by PRF 85, PRF 65 and at last PRF 0. The velocities needed for lift up decreased as the equivalence ratio increased. Air flow being the controlling factor of different equivalence ratios, it was deduced that lower mixture velocities corresponding to higher equivalence ratios required less amounts of secondary gas velocities for lift up and higher mixture velocities at low equivalence ratios required higher secondary gas velocities. Higher decreasing slope was seen for quenching velocities with helium versus equivalence ratios. Helium gas was able to lift both PRF 0 and 100 flames at much lower equivalence ratios compared to nitrogen. The difference in velocities needed to lift up different octane number flames was much lower with helium than nitrogen.

Finally, gasoline fuels with octane number of 87 and 91 were tested that validated the quenching method for octane number determination. It was determined that difference between different octane number fuels including gasoline as well as PRF fuels was distinguishable between equivalence ratios of 1.8 to about 2.4 that was based on the required quenching velocities needed for liftoff. It is recommended that premixed flame

experiments of fuel air mixtures between the equivalence ratios of 1.8 and 2.4 be considered for octane number determination. Different amount of quenching velocities of nitrogen gas needed for liftoff of the flame can help determine a fuel's octane number. However, it should be noted that the proposed new method needs to be calibrated for specific fuel sources, distillation processes, and octane enhancers used. In conclusion, the experimental results support the hypothesis that flame quenching can be correlated to fuel mixture octane number, and holds potential as an alternative method to determine the octane number.

REFERENCES

- "CHEMKIN." Reaction Design. 2008. Reaction Design. Mar. 2008
- C. K. Law, "*Dynamics of stretched flames*", The Combustion Institute, 1988, pp. 1381-1402
- C. Liu, B. Yan, G. Chen, X.S. Bai, "*Structures and burning velocity of biomass derived gas flames*", International Journal of Hydrogen Energy 35 (2009) 542-555
- C. Meneveau and T. Poinso, "*Stretching and quenching of flamelets in premixed turbulent combustion*", Combustion and Flame 86, 1991, 311-322
- D. Bradley, M. Lawes, Kexin Liu, R. Woolley, "*The quenching of premixed turbulent flames of iso-octane, methane and hydrogen at high pressures*", Proceedings of the Combustion Institute 31 (2007) 1393-1400
- E. W. Kaiser, J. Platz, H.J. Curran, "*Experimental and Modeling Study of Premixed Atmospheric-Pressure Dimethyl Flames*", J. Phys. Chem. A 2000, 104, 8194-8206
- Emanuel S. Stockman, Sohail H. Zaidi, Richard B. Miles, Campbell D. Carter, Michael D. Ryan, "*Measurements of combustion properties in a microwave enhanced flame*", Combustion and Flame 156 (2009) 1453-1461
- F. Migliorini, S. De Iuliis, F. Cignoli, G. Zizak, "*How 'flat' is the rich premixed flame produced by your McKenna burner*", Combustion and Flame, 2008
- G Hartung, J Hult and C F Kaminski, "*A flat flame burner for the calibration of laser thermometry techniques*", Measurement Science and Technology 17 (2006) 2485-2493
- George E. Totten, Steven R. Westbrook, Rajesh J. Shah, "*Fuels and lubricants handbook*", pp. 61 – 88, 2003
- Graham Dixon-Lewis, "*Laminar premixed flame extinction limits I- Combined effects of stretch and upstream heat loss in the twin-flame unburnt-unburnt opposed flow configuration*", Mathematical, Physical and Engineering Sciences, Vol. 452, No, 1951 (August 1996)
- Holthuis & Associates, McKenna Flat Flame Burner manufacturer, Sebastopol, CA
- Jun'ichi Sato, "*Effects of Lewis number on extinction behavior of premixed flames in a stagnation flow*", The Combustion Institute, 1982, pp. 1541-1548
- M. P. Halstead, A. Prothero, C. P. Quinn, "*A Mathematical model of the cool-flame oxidation of acetaldehyde*", Royal Society of London, Series A, Mathematical and Physical Sciences, Vol. 322, No. 1550. (1971), pp. 377-403

Neal Morgan, Andrew Smallbone, Amit Bhave, Markus Kraft, Roger Cracknell, Gautam Kalghatgi, “*Mapping surrogate gasoline compositions into RON/MON space*”, *Combustion and Flame* 157 (2010) 1122-1131

P.R. Ballinger, P.R. Ryason, “*Isolated stable cool flames of hydrocarbons*”, Chevron Research Company, 2007

Reaction Design. Theory Manual - CHEMKIN Software. Release 4.0.1. 2004

R.G. Abdel-Gayed, D. Bradley and M. Lawes, “*Turbulent burning velocities: a general correlation in terms of straining rates*”, *The Royal Society*, Vol. 414, No. 1847 (December 1987), pp. 389-413

R. Meusinger, R. Moros, “*Determination of octane numbers of gasoline compounds from their chemical structure by CNMR spectroscopy and neural networks*”, Elsevier Science Ltd., 2000

S. Cheskis, A. Goldman, “*Laser diagnostics of trace species in low-pressure flat flame*”, *Progress in Energy and Combustion Science* 35 (2009) 365-382

S. I. Yang and S. S. Shy, “*Global quenching of premixed CH_4 /Air flames: Effects of turbulent straining, equivalence ratio, and radiative heat loss*”, *The Combustion Institute*, Vol. 29 (2009), pp. 1841-1847

Ya. Yu. Stepankii, N. P. Evmeneko, G. S. Yablonskii and B. I. Kusovskii, “*Correlation between octane number and certain parameters*”, *Chemistry and technology of fuels and oils*, 1980, Vol. 16, Number 8, pp. 554-557